AD

MODELING OF THE NON-AUDITORY RESPONSE TO BLAST OVERPRESSURE

Calculation of the Internal Mechanical Response of Sheep to Blast Loading

ANNUAL/FINAL REPORT

Michael J. Vander Vorst
James H. Stuhmiller

JANUARY 1990

Supported by

U.S. ARMY MEDICAL RESEARCH AND DEVELOPMENT COMMAND
Fort Detrick, Frederick, Maryland 21701-5012

Contract No. DAMD17-8[illegible]-C-5238

JAYCOR
11011 Torreyana Road
San Diego, California 92121-1190

MODELING OF THE NON-AUDITORY RESPONSE TO BLAST OVERPRESSURE

Calculation of the Internal Mechanical Response of Sheep to Blast Loading

JANUARY 1990

Supported by

U.S. ARMY MEDICAL RESEARCH
AND DEVELOPMENT COMMAND
Fort Detrick
Frederick, Maryland 21701-5012

Contract No. DAMD17-85-C-5238

Research was conducted according to the principles enunciated in the "Guide for Laboratory Animal Facilities and Care," prepared by the National Academy of Sciences--National Research Council. This work is supported in part by the U.S. Army Medical Acquisition Activity, contract number DAMD 17-85-C-5238. The views, opinions and/or findings contained in this report are those of the authors and should not be construed as an official Department of the Army position, policy or decision unless so designated by other documentation.

REPORT DOCUMENTATION PAGE

1a. REPORT SECURITY CLASSIFICATION Unclassified	1b. RESTRICTIVE MARKINGS N/A
2a. SECURITY CLASSIFICATION AUTHORITY N/A	3. DISTRIBUTION / AVAILABILITY OF REPORT Approved for Public Release; Distribution unlimited
2b. DECLASSIFICATION / DOWNGRADING SCHEDULE N/A	
4. PERFORMING ORGANIZATION REPORT NUMBER(S)	5. MONITORING ORGANIZATION REPORT NUMBER(S)
6a. NAME OF PERFORMING ORGANIZATION JAYCOR Applied Sci. & Engr. Technol. Group 6b. OFFICE SYMBOL (If applicable)	7a. NAME OF MONITORING ORGANIZATION Director Walter Reed Army Institute of Research
6c. ADDRESS (City, State, and ZIP Code) 11011 Torreyana Rd. San Diego, CA 92121-1190	7b. ADDRESS (City, State, and ZIP Code) ATTN: SGRD-UWZ-C, Kenneth T. Dodd, Ph.D. Bldg. 40 Washington, DC 20307-5100
8a. NAME OF FUNDING / SPONSORING ORGANIZATION U. S. Army Medical Res. & Devel. Cmd. 8b. OFFICE SYMBOL (If applicable)	9. PROCUREMENT INSTRUMENT IDENTIFICATION NUMBER DAMD17-85-C-5238
8c. ADDRESS (City, State, and ZIP Code) Fort Detrick Frederick, MD 21701-5012	10. SOURCE OF FUNDING NUMBERS PROGRAM ELEMENT NO. 62787A; PROJECT NO. 62787A878; TASK NO. AB; WORK UNIT ACCESSION NO. 004

11. TITLE (Include Security Classification)

(U) Modeling of the Non-Auditory Response to Blast Overpressure

12. PERSONAL AUTHOR(S) Michael J. Vander Vorst and James H. Stuhmiller

13a. TYPE OF REPORT	13b. TIME COVERED	14. DATE OF REPORT (Year, Month, Day)	15. PAGE COUNT
Annual/Final	FROM 8/15/85 TO 7/31/89	1990 January	68

16. SUPPLEMENTARY NOTATION

Calculation of the Internal Mechanical Response of Sheep to Blast Loading

17. COSATI CODES			18. SUBJECT TERMS (Continue on reverse if necessary and identify by block number)
FIELD	GROUP	SUB-GROUP	RA 3, Numerical Analysis, Differential Equations, Weapons Effects, Biomechanics, Blast Injuries, Non-Auditory, Response to Blast Overpressure
26	14		
23	04		

19. ABSTRACT (Continue on reverse if necessary and identify by block number)

Calculations are made of the intrathoracic pressure expected from blast loading of sheep. A mathematical model of the chest wall and lung parenchyma have been formulated as a system of differential equations which include the effects of chest wall mass and resistance, density of the parenchyma and an adiabatic equation of state for air within the parenchyma. The differential equations are discretized as a system of nonlinear finite difference equations with the blast loading appearing as a boundary condition. This finite system is then solved on a computer using an implicit solution algorithm. Blast loadings used in the calculations are from field tests and correspond to animal response ranging from no injury to severe injury. Intrathoracic pressure in the esophagus and at four locations within the lung parenchyma, all in the approximate plane of the seventh thoracic vertebra, are compared with field test measurements for four occupational levels and four injury levels of blast overpressure.

20. DISTRIBUTION / AVAILABILITY OF ABSTRACT ☐ UNCLASSIFIED/UNLIMITED ☒ SAME AS RPT. ☐ DTIC USERS	21. ABSTRACT SECURITY CLASSIFICATION Unclassified
22a. NAME OF RESPONSIBLE INDIVIDUAL Mary Frances Bostian	22b. TELEPHONE (Include Area Code) [301] 663-7325 22c. OFFICE SYMBOL SGRD-RMI-S

DD FORM 1473, 84 MAR

19. ABSTRACT *(Continued from front)*

CALCULATION OF THE INTERNAL MECHANICAL RESPONSE OF SHEEP TO BLAST LOADING

Michael J. Vander Vorst
Applied Science and Engineering Technology
JAYCOR

ABSTRACT

Calculations are made of the intrathoracic pressure expected from blast loading of sheep. A mathematical model of the chest wall and lung parenchyma have been formulated as a system of differential equations which include the effects of chest wall mass and resistance, density of the parenchyma and an adiabatic equation of state for air within the parenchyma. The differential equations are discretized as a system of nonlinear finite difference equations with the blast loading appearing as a boundary condition. This finite system is then solved on a computer using an implicit solution algorithm. Blast loadings used in the calculations are from field tests and correspond to animal response ranging from no injury to severe injury. Intrathoracic pressure in the esophagus and at four locations within the lung parenchyma, all in the approximate plane of the seventh thoracic vertebra, are compared with field test measurements for four occupational levels and two injury levels of blast overpressure.

CONTENTS

ILLUSTRATIONS

TABLES

INTRODUCTION

Evidence of acute thoracic injury in animals from intense blast overpressure exposure and the possibility of chronic injury to crew from the blasts of conventional weapons have prompted the need for detailed mathematical models of the thorax. The ultimate model may be a three-dimensional representation of the thoracic cavity, however an understanding of the key physical processes taking place in the thorax is more economically gained through simpler one-dimensional models. Since field tests using sheep show that the thoracic organ sustaining the most injury is the lung, a one-dimensional model of a cross section of a sheep thorax was constructed. This model includes ribs, lung parenchyma and the esophagus.

Field tests, using small conventional explosives at six blast conditions, have been conducted on sheep instrumented with pressure gauges in the lung and the esophagus.[1] Free field and face-on reflected pressures were also recorded. Hence both the pressure loading on the sheep's ribs and the resulting pressure within the thorax are known for these cases. Calculations with the one-dimensional model using the measured loads from the field tests are compared to the measured intrathoracic pressures.

The remainder of this paper presents the one-dimensional mathematical model of the thorax and the numerical method used to solve the resulting equations. Finally, comparisons of the results of the model with field test data are made and conclusions are drawn.

MODEL

An illustration of a cross-section of a sheep's thorax at the seventh thoracic vertebrae is shown in Figure 1. The geometry modeled is indicated by the horizontal line, also shown in Figure 1, just below the seventh thoracic vertebrae of the animal. This line extends from the right rib surface into the right lung lobe through the esophagus into the left lung lobe and finally to the left rib surface.

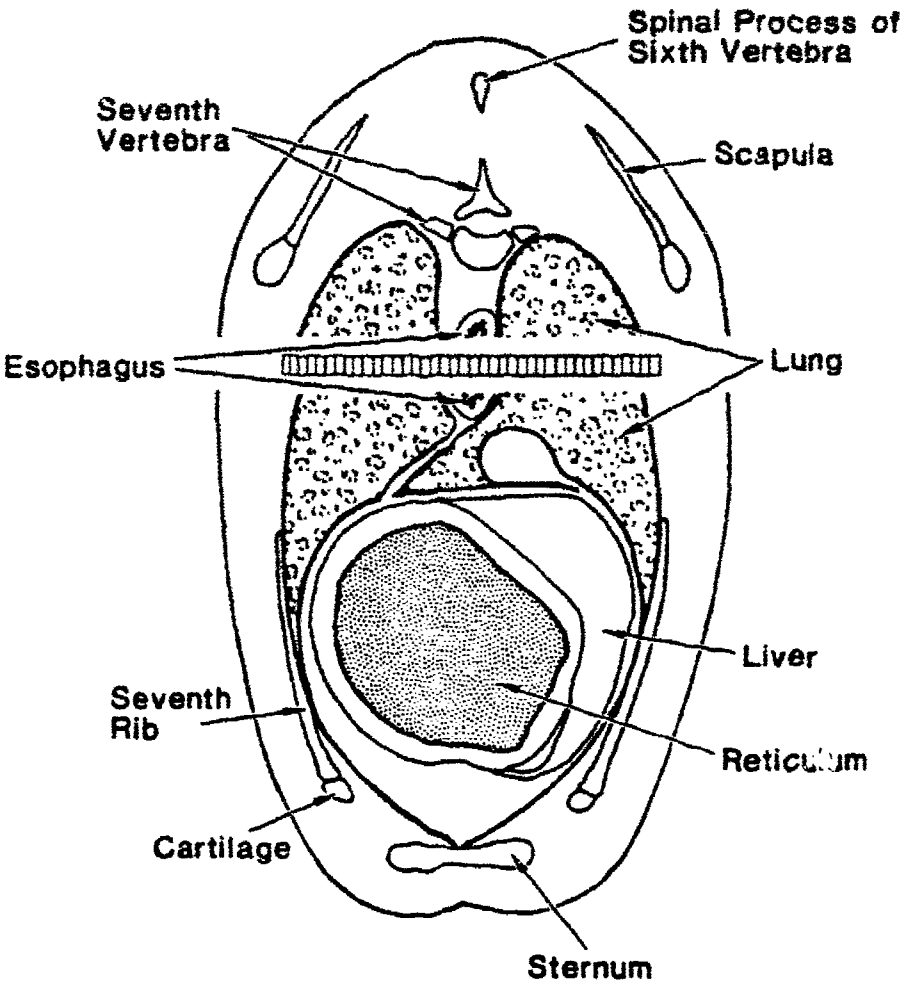

Figure 1. Anatomical cross section at level of seventh thoracic vertebra showing one-dimensional computational domain.

The finite model for this one-dimensional cross-section of the thorax is indicated in Figure 2. The model is one of point masses, M_i, which represent either the parenchymal tissue or rib/muscle. The point masses are separated by finite cells of air with volume V_i. Since this is a macroscopic model whose purpose is to predict the mechanical response of the lung, the length of the air cells in the model is much larger than the diameter of individual alveoli. The size of the air cells is determined heuristically to adequately resolve the pressure wave induced by the blast loading. The right and left rib surfaces are loaded with the measured pressures, $P_r(t)$ and $P_l(t)$, respectively.

In a typical field test shown in Figure 3, a conventional charge of weight, W, is exploded at a height of burst, HOB, above the ground. The test subject is located a horizontal distance, R, from the charge. In all cases the range, R, of the animal from the charge is beyond the Mach reflection distance and the triple point of the Mach stem is above the animal. The animal is oriented so that the Mach stem strikes orthogonally on its right side. The blast overpressure displaces the chest wall which in turn displaces the lung and sets up a pressure wave moving through the lung parenchyma.

A model of the motion of the chest wall and lung is given by a system of differential equations. The motion of each of the masses, M, is governed by the momentum equation:

$$M \frac{\partial u}{\partial t} + Cu + kx = \Delta p \cdot A \qquad (1)$$

where

$$u = \frac{\partial x}{\partial t} \qquad (2)$$

and

$$V = V^0 + \Delta(Ax) \quad . \qquad (3)$$

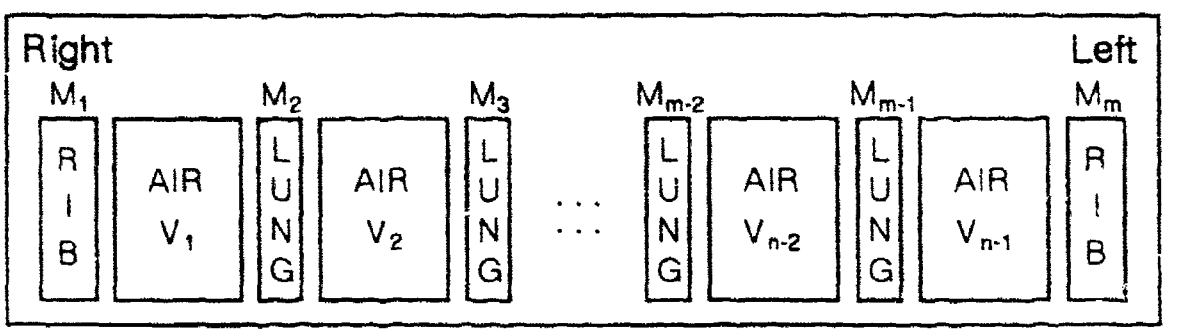

Figure 2. Schematic of the Lung Model

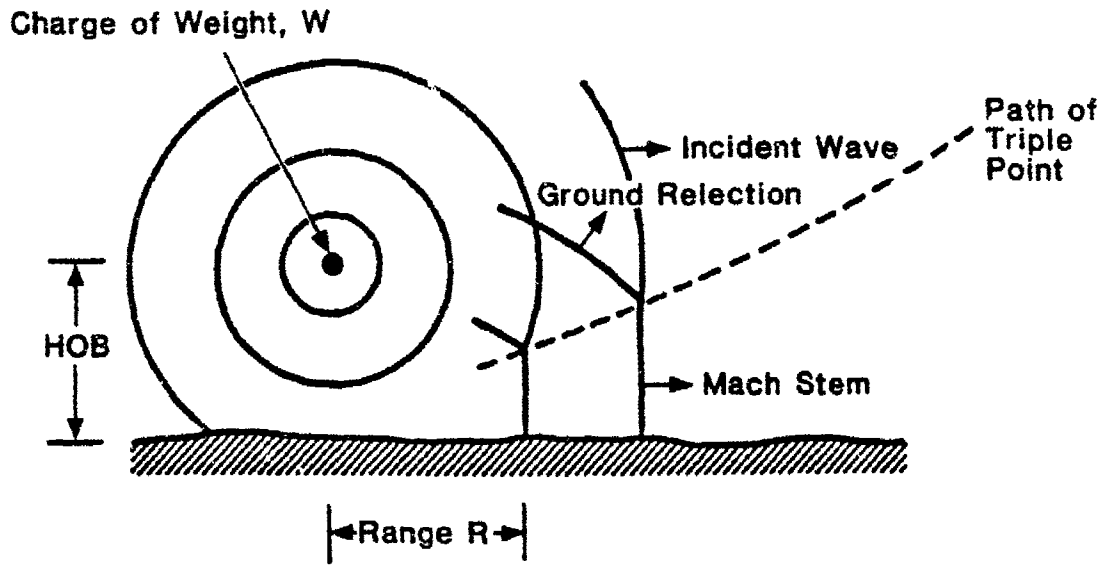

Figure 3. Blast parameters.

In this analysis, x is displacement, t is time, u is velocity, C is the damping coefficient and k is the spring constant. The pressure, p, in the lung is given by the adiabatic equation of state in terms of the volume, V, by

$$p = p^0\left[V^0/V\right]^\gamma \tag{4a}$$

$$V = V^0 + \Delta V \tag{4b}$$

$$\Delta V = \Delta(Ax) \tag{4c}$$

where the superscript, 0, indicates initial values.

On the right and left chest wall, the pressure is prescribed by the external loads as

$$p_r = p_r(t) \tag{5a}$$

$$p_l = p_l(t) \tag{5b}$$

For the cases under consideration, the loading functions p_r and p_l are from measured data.[1]

NUMERICAL METHOD

The system of equations, Eq. 1 through Eq. 5, are discretized using an implicit formulation as

$$M_i \frac{u_i^{n+1} - u_i^n}{\partial t} + k_i x_i^{n+\frac{1}{2}} + C_i u_i^{n+\frac{1}{2}} = \left[p_{i+1}^{n+\frac{1}{2}} - p_i^{n+\frac{1}{2}}\right] A_i^{n+\frac{1}{2}} \tag{6}$$

$$x_i^{n+1} - x_i^n = u_i^{n+\frac{1}{2}} \delta t \tag{7}$$

$$V_i^{n+1} = V_i^0 + \left(A_{i+1}^{n+1} x_{i+1}^{n+1} - A_i^{n+1} x_i^{n+1}\right) \tag{8}$$

$$p_i^{n+1} = p_i^0 \left(V_i^0 / V_i^{n+1}\right)^{\nu} \tag{9}$$

$$x_i^{n+\frac{1}{2}} = \frac{1}{2}\left(x_i^{n+1} + x_i^n\right) \tag{10a}$$

$$p_i^{n+\frac{1}{2}} = \frac{1}{2}\left(p_i^{n+1} + p_i^n\right) \tag{10b}$$

$$u_i^{n+\frac{1}{2}} = \frac{1}{2}\left(u_i^{n+1} + u_i^n\right) \tag{10c}$$

From Eqs. 7 and 8, we have

$$u_i^{n+1} = 2 \frac{x_i^{n+1} - x_i^n}{\partial t} - u_i^n \tag{11}$$

Substituting Eqs. 7, 10, and 11 into Eq. 6, the terms u_i^{n+1}, $u_i^{n+\frac{1}{2}}$, $x_i^{n+\frac{1}{2}}$, and $p_i^{n+\frac{1}{2}}$ are eliminated from the momentum equation in favor of x_i^{n+1}, p_i^{n+1} and known values at the old time level, n, to obtain

$$\left[\frac{2M_i}{\partial t^2} + \frac{1}{2}k_i + \frac{C_i}{\delta t}\right] x_i^{n+1} + \frac{1}{2}\left[p_i^{n+1} - p_{i-1}^{n+1}\right] A_i$$

$$= \left[\frac{2M_i}{\partial t^2} - \frac{1}{2}k_i + \frac{C_i}{\partial t}\right] x_i^n + \frac{2M_i}{\partial t} u_i^n - \frac{1}{2}\left[p_i^n - p_{i-1}^n\right] A_i \qquad (12)$$

where we assume that A_i do not change with time. For the calculations presented here, all A_i are the same. From Equations 8 and 9, the pressure, p_i^{n+1}, is a function of only the displacements x_i^{n+1} and x_{i+1}^{n+1}. Hence, taken over each of the cells, the finite difference momentum equation, Eq. 12, is a system of nonlinear algebraic equations for the nodal displacements, x_i^{n+1}. This system can be written as

$$\alpha_i x_i^{n+1} + \frac{1}{2}\left[p_i^{n+1} - p_{i-1}^{n+1}\right] A_i = \beta_i^n \qquad (13)$$

where

$$\alpha_i = \frac{2M_i}{\partial t^2} + \frac{1}{2}k_i + \frac{C_i}{\partial t} \qquad (14)$$

$$\beta_i^n = \left[\frac{2M_i}{\partial t^2} - \frac{1}{2}k_i + \frac{C_i}{\partial t}\right] x_i^n + \frac{2M_i}{\partial t} u_i^n - \frac{1}{2} A_i \left[p_i^n - p_{i-1}^n\right] \quad . \qquad (15)$$

From Eqs. 4, the value of the pressure at each of the interior nodes, i=2 to i=m−1, is prescribed by

$$p_i^{n+1} = p_i^0 \left[V_i^0\right]^{\gamma} \left[V_i^0 + A_{i+1} x_{i+1}^{n+1} - A_i x_x^{n+1}\right]^{-\gamma} \quad . \qquad (16)$$

At the rib surfaces, i=1 and i=m, the pressure is given by the boundary conditions

$$p_1^{n+1} = p_r\left|t^{n+1}\right| \quad , \qquad (17a)$$

and

$$p_m^{n+1} = p_l\left|t^{n+1}\right| \quad . \qquad (17b)$$

At each time step, the $m-2$ roots,

$$x_i; \quad i=2 \text{ to } m-1$$

of the system of $m-2$ nonlinear algebraic equations

$$R_i(x) = \alpha\, x_i + \frac{1}{2} A_i \left[p_i - p_{i-1} \right] - \beta_i^n \tag{18}$$

must be found. This system is solved by Newton iteration. Let ν be iteration index and for brevity denote the most recent value $[x_i^{n+1}]^\nu$ by x_i^ν. Furthermore, use the known values at the old time level, n, as the initial guess to the new displacements at time $n+1$, that is for $\nu=0$

$$\left[x_i^{n+1} \right]^0 = x_i^n \quad . \tag{18a}$$

Now expand $R(x^{\nu+1})$ in a Taylor series about x^ν as

$$R_i^{\nu+1} = R_i^\nu + \frac{\partial R_i}{\partial x_{i-1}} \delta x_{i-1} + \frac{\partial R_i^\nu}{\partial x_i} \delta x_i + \frac{\partial R_i^\nu}{\partial x_{i+1}} \delta x_{i+1} \tag{19}$$

where

$$x^{\nu+1} = x^\nu + \delta x \quad . \tag{20}$$

Setting, $R_1^{\nu+1} = 0$, in Equation 19 produces the system

$$\frac{\partial R_i^\nu}{\partial x_{i-1}} \delta x_{i-1} + \frac{\partial R_i^\nu}{\partial x_i} \delta x_i + \frac{\partial R_i^\nu}{\partial x_{i+1}} \delta x_{i+1} = - R_i^\nu \tag{21}$$

of linear algebraic equations for δx_i with coefficients

$$\frac{\partial R_i}{\partial x_{i-1}} = - \frac{1}{2} A_i \frac{\partial p_{i-1}}{\partial x_{i-1}}$$

$$\frac{\partial R_i}{\partial x_i} = \alpha + \frac{1}{2} A_i \left(\frac{\partial p_i}{\partial x_i} - \frac{\partial p_{i-1}}{\partial x_{i-1}} \right)$$

$$\frac{\partial R_i}{\partial x_{i+1}} = \frac{1}{2} A_i \frac{\partial p_i}{\partial x_{i+1}}$$

where

$$\frac{\partial p_i}{\partial x_i} = \gamma A_i \frac{p_i}{V_i}$$

$$\frac{\partial p_i}{\partial x_{i+1}} = -\gamma A_i \frac{p_{i-1}}{V_{i-1}} \quad .$$

Finally the coefficients $\partial R/\partial x$ are expressed in terms of most recently known values at iteration level ν as follows:

$$\frac{\partial R_i^{\nu}}{\partial x_{i-1}} = -\frac{1}{2} A_i A_{i-1} \gamma \frac{p_{i-1}^{\nu}}{V_{i-1}^{\nu}} \tag{22a}$$

$$\frac{\partial R_i^{\nu}}{\partial x_i} = \alpha + \frac{1}{2} A_i \gamma \left(A_{i+1} \frac{p_i^{\nu}}{V_i^{\nu}} + A_{i-1} \frac{p_{i-1}^{\nu}}{V_{i-1}^{\nu}} \right) \tag{22b}$$

$$\frac{\partial R_i^{\nu}}{\partial x_{i+1}} = -\frac{1}{2} A_i A_{i+1} \gamma \frac{p_i^{\nu}}{V_i^{\nu}} \tag{22c}$$

for interior cells $i=3$ to $i=m-2$. For the cell, $i=2$, next to the right rib, the coefficients become

$$\frac{\partial R_i^{\nu}}{\partial x_{i-1}} = 0 \tag{23a}$$

$$\frac{\partial R_i^{\nu}}{\partial x_i} = \alpha + \frac{1}{2} A_i A_{i+1} \gamma \frac{p_i^{\nu}}{V_i^{\nu}} \tag{23b}$$

$$\frac{\partial R_i^{\nu}}{\partial x_{i+1}} = -\frac{1}{2} A_i A_{i+1} \gamma \frac{p_i^{\nu}}{V_i^{\nu}} \quad . \tag{23c}$$

For the cell, $i=m-1$, next to the left rib, the coefficients become

$$\frac{\partial R_i^{\nu}}{\partial x_{i-1}} = -\frac{1}{2} A_i A_{i-1} \gamma \frac{p_{i-1}^{\nu}}{V_{i-1}^{\nu}} \tag{24a}$$

$$\frac{\partial R_i^{\nu}}{\partial x_i} = \alpha + \frac{1}{2} A_i A_{i-1} \gamma \frac{p_{i-1}^{\nu}}{V_{i-1}^{\nu}} \tag{24b}$$

$$\frac{\partial R_i^{\nu}}{\partial x_{i+1}} = 0 \quad . \tag{24c}$$

To summarize, the solution algorithm is to initialize the Newton iteration using the old values

$$\left(x_i^{n+1}\right)^0 = x_i^n \quad ,$$

calculate the residual, R^{ν}, solve the tridiagonal system of linear algebraic equations, Eq. 21, update the displacements using Eq. 20 and finally calculate the new residual R at iteration $\nu+1$. The iteration is stopped when the residual becomes less than some prescribed value, ε, which is based upon the precision of the machine. For computer systems with 64 bit floating point arithmetic, convergence is usually obtained in three or four iterations with an ε value of 10^{-6}.

These finite difference equations, with the solution procedure outlined above, were implemented as algorithms in the computer program, THOR, to numerically model the mechanical response of the thorax to blast loading. In summary, THOR is a one-dimensional, Lagrangian, compressible flow computer program which utilizes a finite treatment of the lung mass and an adiabatic equation of state for the air within the lung.

LABORATORY TESTS

A blast loading applied to the chest wall of an animal produces a displacement of the chest wall which in turn sets up a compression wave in the lung. Succeeding sections of this paper will present comparisons of calculated results of the pressure in the lung using the THOR computer program with in-vivo measurements in sheep lung taken by Dodd.[1,2] However the lung is a complex geometry and it is impossible to see a wave propagate within it. Additionally, THOR is a single-dimensional model, while the lung is clearly three-dimensional. Hence the adequacy of the one-dimensional assumption of wave propagation and the applicability of the mathematical models in THOR must be resolved before comparison of THOR calculations with the in-vivo measurements can be trusted. In order to learn more about the propagation properties of these waves in a simpler controlled environment, Yu, Ho and Stuhmiller[3] constructed a surrogate thorax. This surrogate thorax is an acrylic tube filled with shaving cream dispensed from a pressurized container. As shown in Figure 4, one end of the tube contains a free moving acrylic block which simulates the chest wall. A shock tube was used to apply a load to the acrylic block. Wave propagation tests using this setup show that shaving cream is a reasonable surrogate for lung tissue. Both parenchymal tissue and shaving cream have a density of about 0.1 g/cm^3 and a wave speed of about 30 m/sec.

Using blast loadings from laboratory tests as input, the THOR computer program was used to calculate the motion of the acrylic block and the pressure in the shaving cream just behind the block. The parameters used for the calculations are as follows:

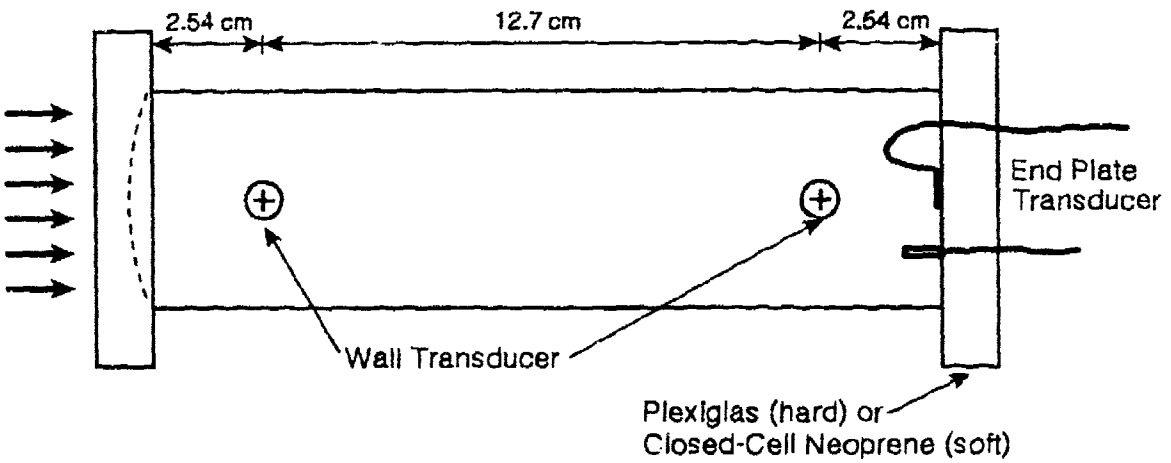

Figure 4. Surrogate thorax.

Chest Wall Mass:	2.5 g/cm^2
Parenchyma density:	0.1 g/cm^3
Rib spring constant:	0.0
Lung damping coefficient:	10.0
Lung width:	15.0 cm
Computational cell size:	0.25 cm

Figures 5 and 6 give a comparison between the THOR calculation and the laboratory tests using the thorax surrogate under two different blast loads. In both cases, the measured peak acceleration is only about one third that of the calculation. However since the the peak velocities obtained by integrating the accelerations agree to within ten percent, it is likely that the experimental error in the peak acceleration is probably large. This hypothesis is reinforced by comparing the measured velocity calculated from:

$$M_r v = M_r \int a_r \, dt = \int \left(p_r - p_\ell \right) dt \tag{25}$$

to the velocity computed by THOR. In Eq. 25, M_r is the chest wall mass per unit surface area, a_r is the chest wall acceleration, p_r is the load, and p_ℓ is the pressure in the lung. These velocities are in good agreement. The computed and measured pressure just behind the surrogate chest wall are also in fair agreement for both blast loading cases.

Yu, et al. also made laboratory tests to measure the dissipation properties of the surrogate material. The test setup uses a 1.5 meter long, 5 cm diameter, cylindrical acrylic pipe. The ends of the tube were clamped with a flexible neoprene membrane. One end of the tube was exposed to the exit of a shock tube. THOR calculations using these conditions revealed that the dissipation experiment differed from the previous test not only by the length of the tube and the mass of the chest wall, but the neoprene exhibited a definite springiness. The parameters finally arrived at for the these calculations are:

Chest Wall Mass:	0.05 g/cm^2
Parenchyma density:	0.1 g/cm^3
Rib spring constant:	10^6
Lung damping coefficient:	10.0
Lung width:	60.0 cm
Computational cell size:	1.0 cm

The comparison between the measured and calculated pressures in the shaving cream are shown in Figure 7. They are in excellent agreement.

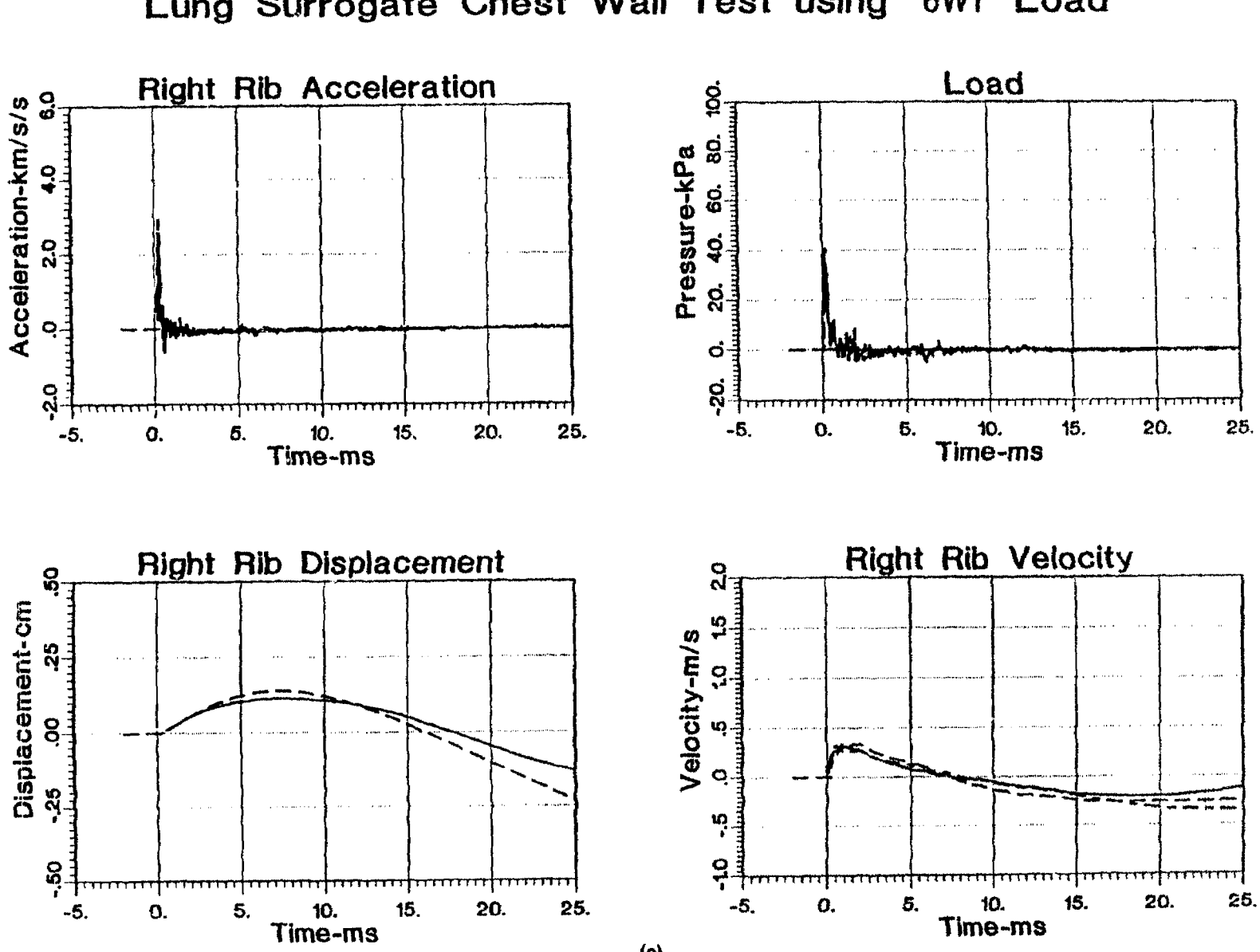

(a)

Figure 5. Comparison of Calculations and Measurements of Surrogate Thorax 40 kPa Load Pressure

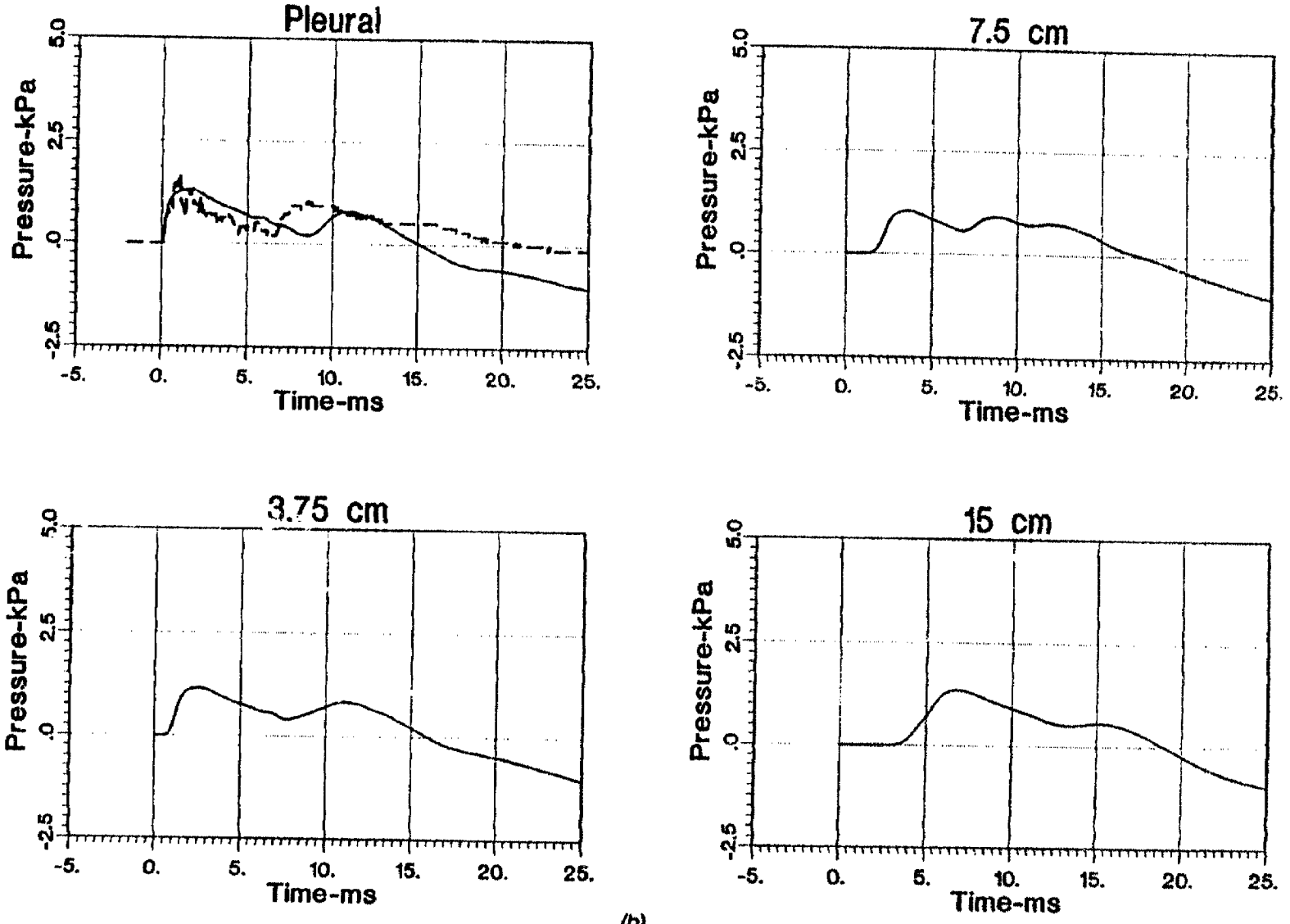

(b)

Figure 5. (Cont'd).

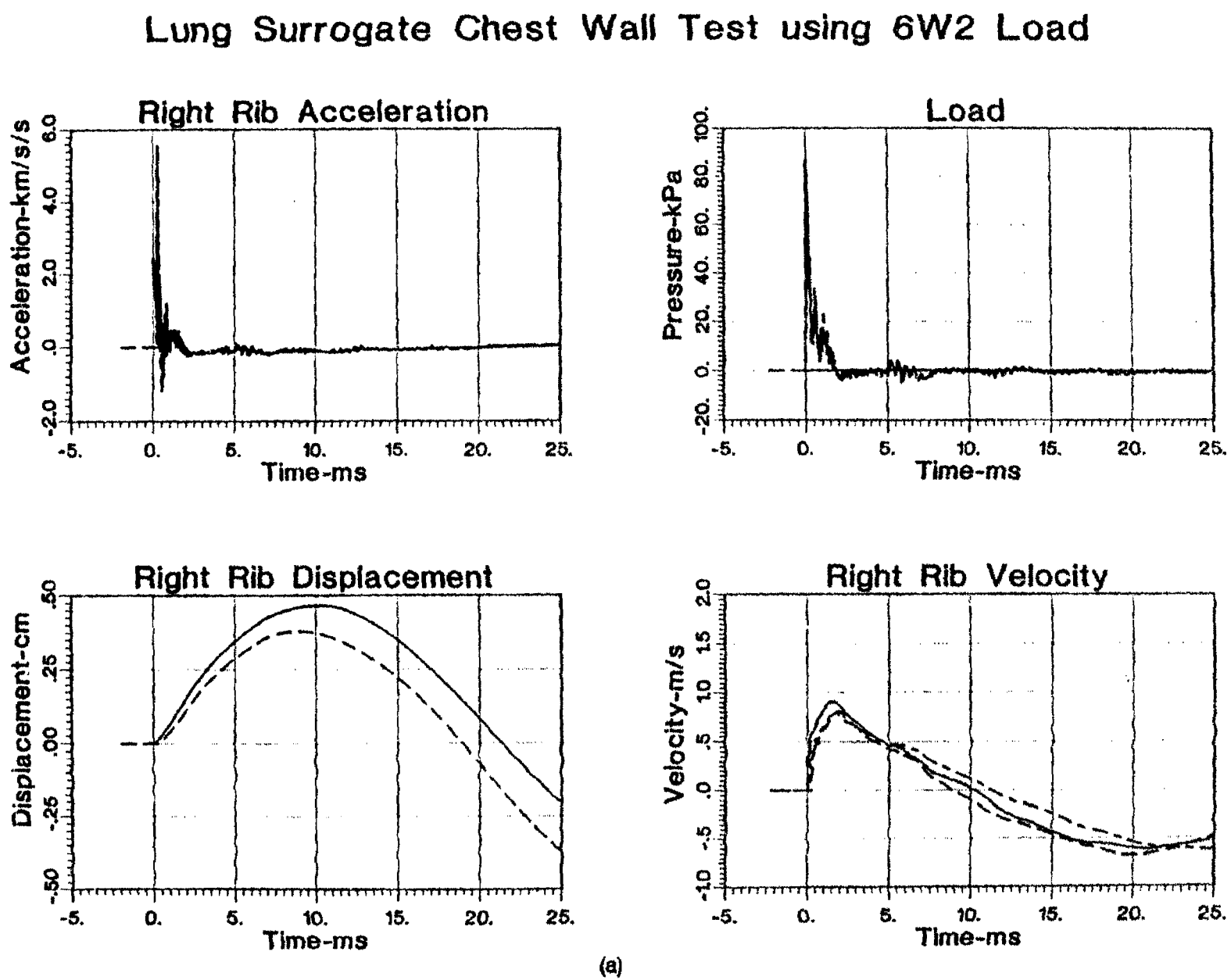

(a)

Figure 6. Comparison of Calculations and Measurements of Surrogate Thorax 80 kPa Load Pressure

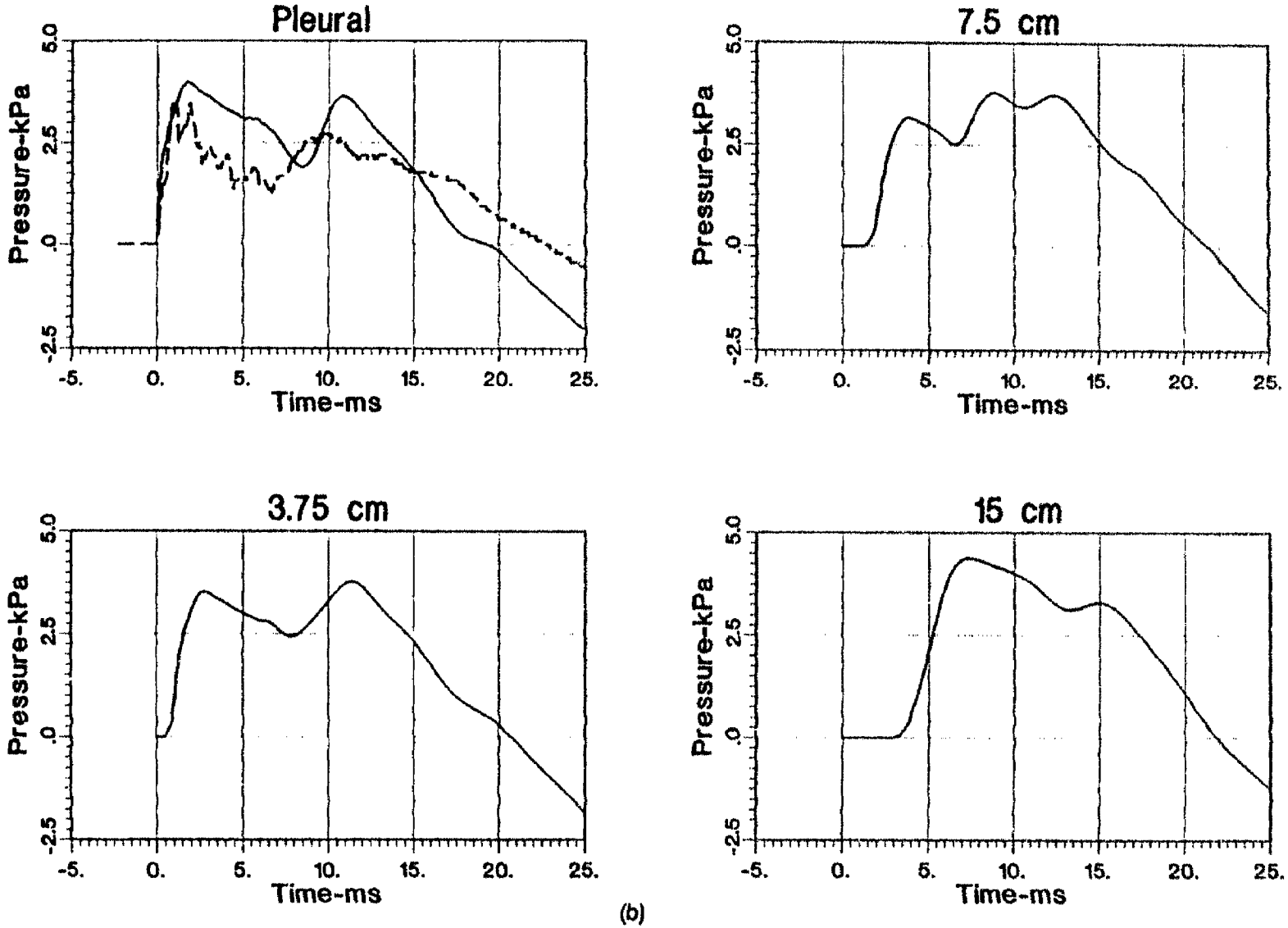

(b)

Figure 6. (Cont'd).

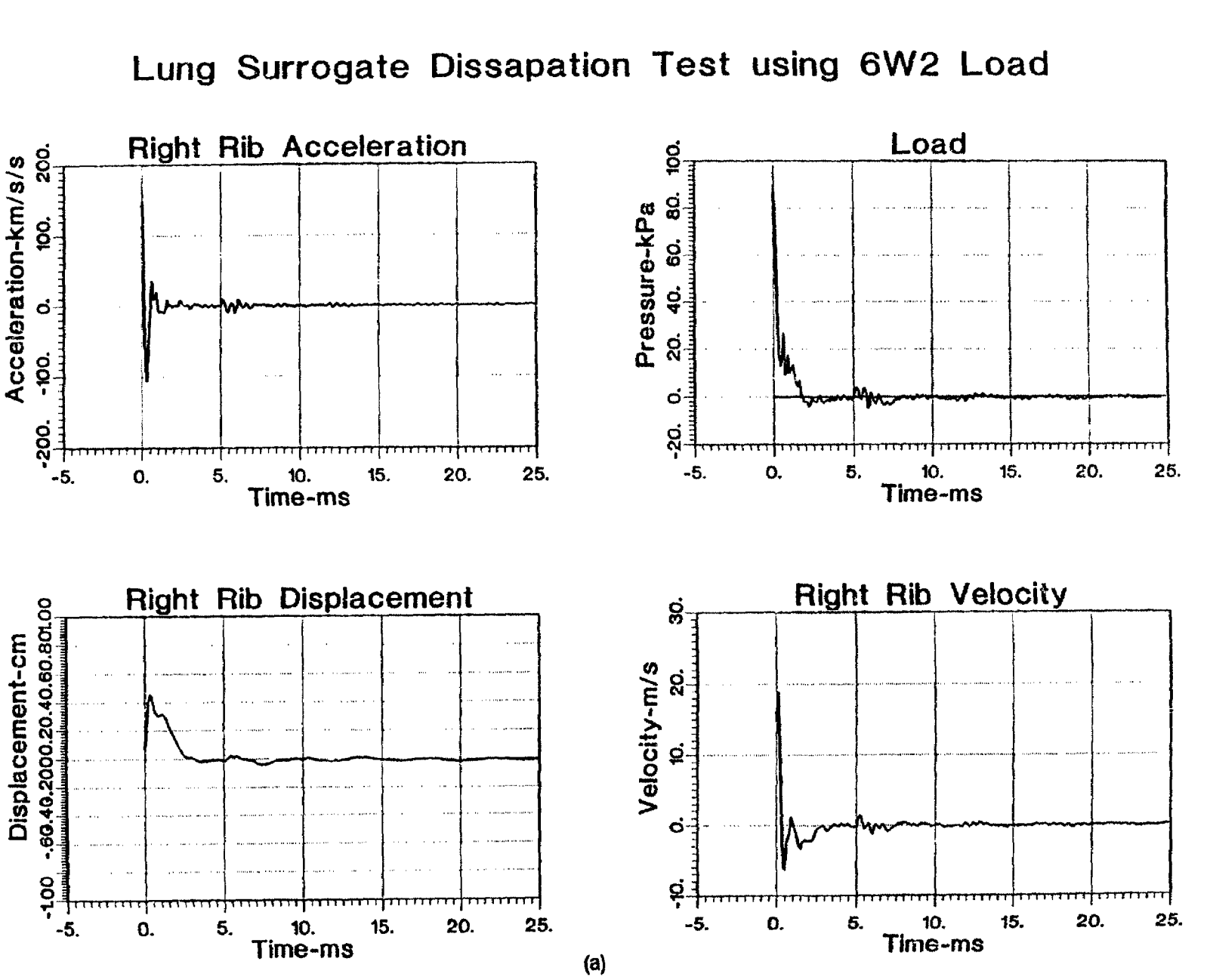

Figure 7. Comparison of Calculations and Measurements of Dissipation in Surrogate Lung. 80 kPa Load Pressure

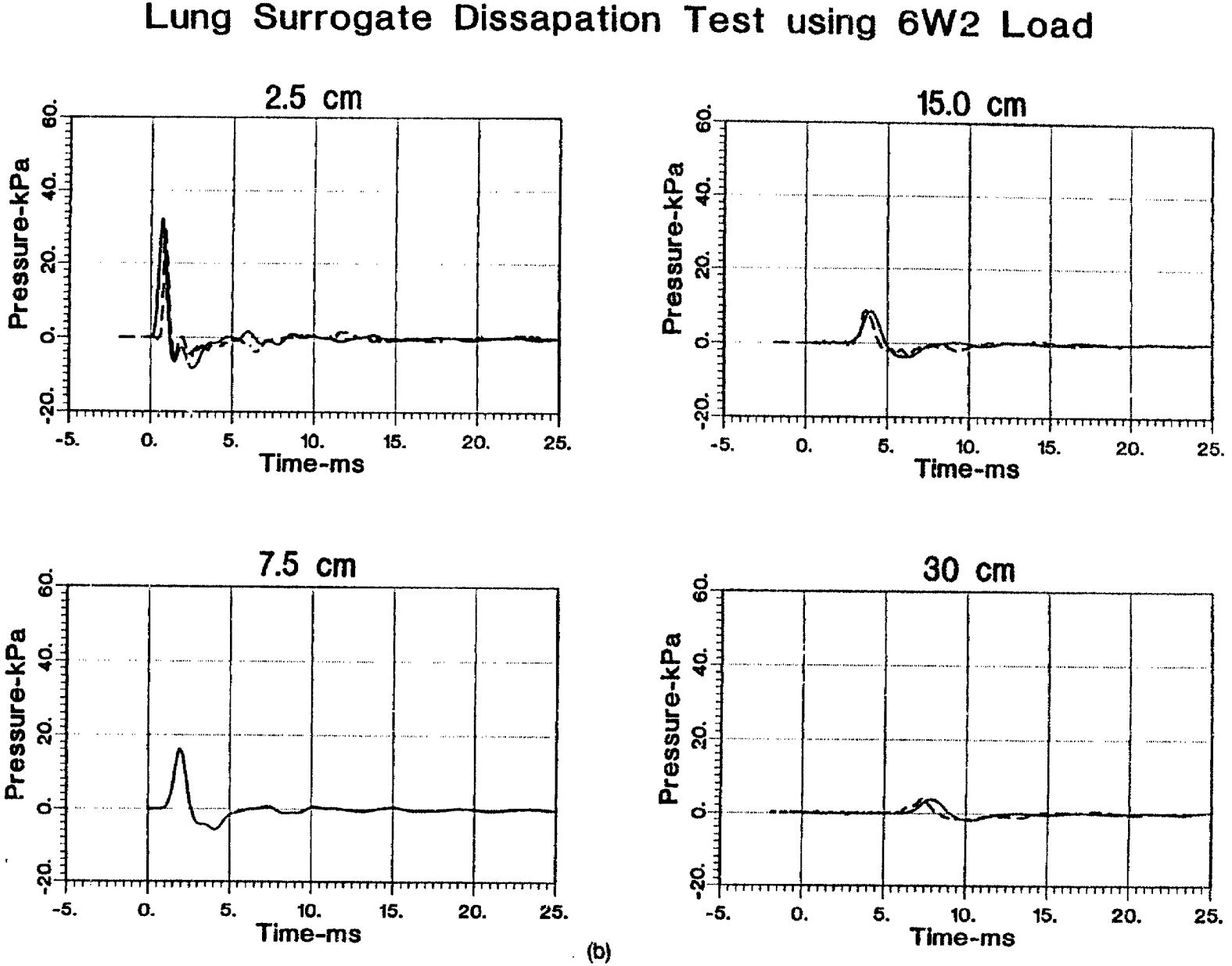

(b)

Figure 7. (Cont'd).

THOR calculations of the response of the surrogate thorax are in good agreement with laboratory measurements. Hence the formulation of the mathematical models and numerical methods used in THOR are valid to simulate wave propagation through a multiple material medium. In addition, Yu's experiments show that the shaving cream behaves like the lung in terms of density and wave speed. The laboratory results using the lung surrogate also suggest that parenchymal material is dissipative. Comparisons, presented in the next section, of THOR calculations with field tests using sheep further reinforce that hypothesis.

FIELD TESTS

Measurements of the thoracic response of sheep to blast loading taken by Dodd[1,2] in the summers of 1985, 1986 and 1987 were reduced to eight cases corresponding to eight different free field blast conditions characterized by charge weight, explosive, range and height of burst. For each case, one representative sample was selected from all the accumulated data for free field pressure, load, rib acceleration, four parenchymal pressure locations and esophageal pressure. This information was placed in VU[5] databases for easy access by the THOR computer program. Most of the load data was obtained from side-on gauges mounted on a rigid, cylindrical test fixture called Lambdroid.[4]

Figure 3 shows the experimental setup in terms of the blast parameters of charge weight, W, range, R, and height of burst, HOB. Each sheep was oriented so that the Mach stem of the blast wave struck the right rib cage of the animal at a right angle. As the blast wave passed over the animal, the right side bore the largest load since it is faced the blast, the top (spine) and bottom (sternum) felt a load approximated by the free field pressure and the left side which is protected sustained the smallest load.

Table 1 presents the eight different blast conditions and Table 2 gives the incident (free field) and reflected (load) blast wave peak pressure, impulse and positive duration at a range corresponding to the right rib cage, side facing the blast, of the sheep for each of the eight cases.

Instrumentation on the sheep were as nearly as possible placed in the location of the seventh thoracic vertebrae along a horizontal line passing through the esophagus. Up to four pressure gauges were placed in the lung parenchyma through the trachea, two each in the right and left lobes, one in the center of each lobe and one near the pleural surface. A hydrophone type pressure gauge was also placed in the esophagus. An accelerometer oriented orthogonally was mounted at the center of the seventh rib. Body surface loading was measured by pressure gauges placed on an anthropomorphic shape, LAMBDROID,[4] placed the same distance from the charge as the sheep. In addition incident free field pressure was taken at the same range. Table 3 gives the location of each of the pressure gauges within the lung and the chest wall mass per unit area used in the calculations.

Figures 8 through 15 present both the measured time traces for each of the eight cases and the calculations using the THOR program. The measured values are shown using dashed lines.

Table 1. Blast Conditions and Injury Levels for Eight Cases

Case	Weight (lb)	HOB (ft)	Range (ft)	Explosive	Injury Level
1	3.0	3.6	16.1	C-4	None
2	3.0	3.0	10.7	C-4	Moderate
3	1.0	0.8	5.6	C-4	Severe
4	0.5	1.0	5.8	C-4	Moderate
5	8.0	3.0	13.2	C-4	Severe
6	8.0	2.0	8.9	C-4	
7	64.0	6.0	30.0	TNT	Moderate
8	8.0	2.0	9.5	C-4	

Table 2. Blast Wave Characteristics at Animal

Case	P_s (kPa)	T_s (ms)	I_s (kPa-ms)	P_r (kPa)	T_r (ms)	I_r (kPa-ms)
1	70	2.7	73	201	2.3	148
2	176	2.1	113	612	1.7	280
3	321	0.8	69	1370	0.8	279
4	160	0.8	47	628	0.9	166
5	227	2.5	167	760	2.0	373
6	643	2.5	287	2900	0.3	368
7	143	6.1	291	511	2.7	404
8	556	2.4	281	2600	0.43	370

Table 3. Lung Width, Probe Locations and Estimated Chest Wall Mass

Case	Width (cm)	RP (cm)	RC (cm)	IEP (cm)	LC (cm)	LP (cm)	M_r (g/cm^2)
1	14.7	0.3	3.0	4.8	11.0	14.3	1.5
2	15.0	1.0	4.0	7.5	11.0	14.0	1.0
3	15.6	0.6	3.0	6.1	11.0	14.4	0.7
4	15.0	1.0	4.0	7.5	11.0	14.0	1.0
5	15.0	0.1	3.7	5.9	12.7	14.4	1.0
6							1.0
7	15.6	0.1	2.0	4.0	10.1	15.0	1.0
8							1.0

Width: *Distance from right to left pleural surfaces*
RP: *Location of Right Pleural pressure transducer*
RC: *Location of Right Center pressure transducer*
IEP: *Location of Esophageal pressure transducer*
LC: *Location of Left Center pressure transducer*
LP: *Location of Left Pleural pressure transducer*
M_r: *Chest wall Mass per unit surface area*

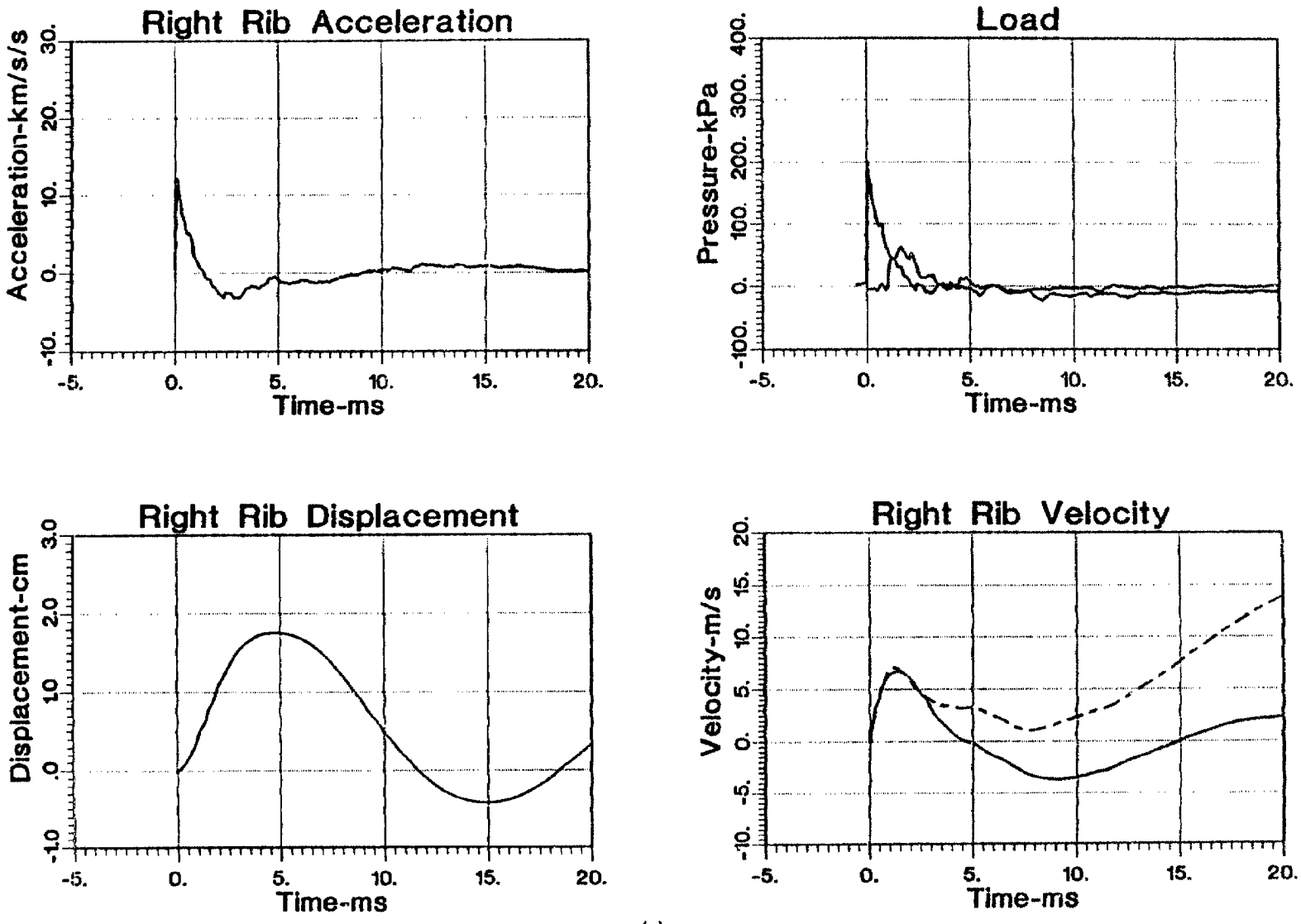

(a)

Figure 8. Case 1 Data Comparison

Freefield Shot: 3 lb C-4 at 3.6 ft HOB and 16.1 ft Range

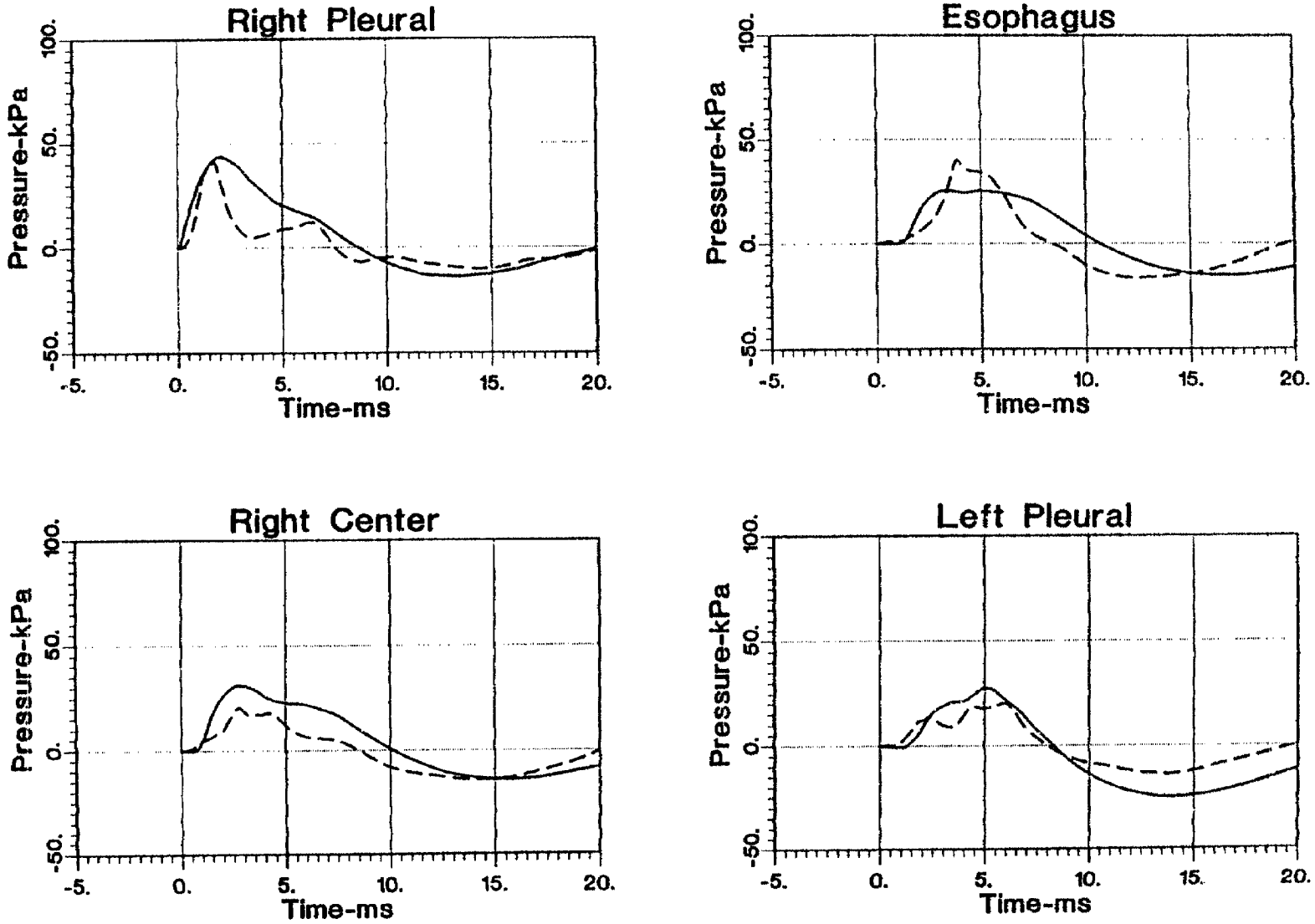

(b)

Figure 8. (Cont'd).

Freefield Shot: 3 lb C-4 at 3.0 ft HOB and 10.7 ft Range

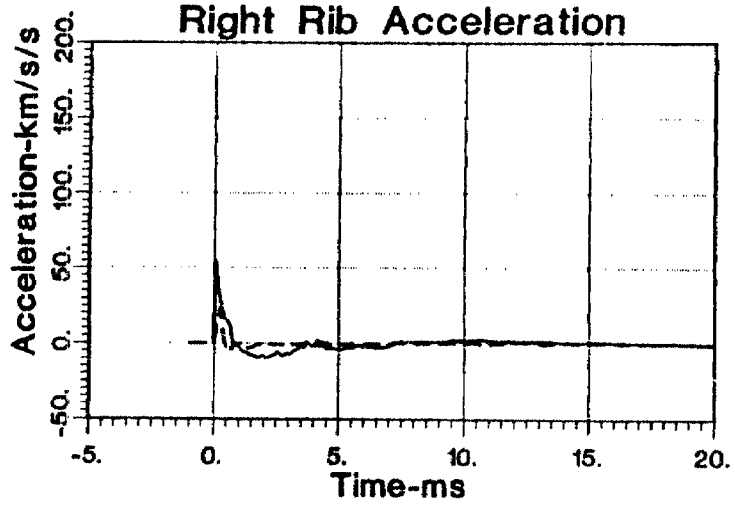

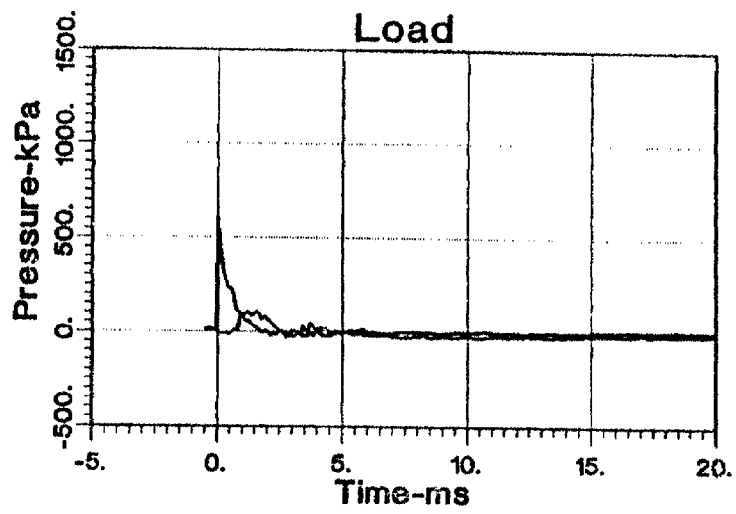

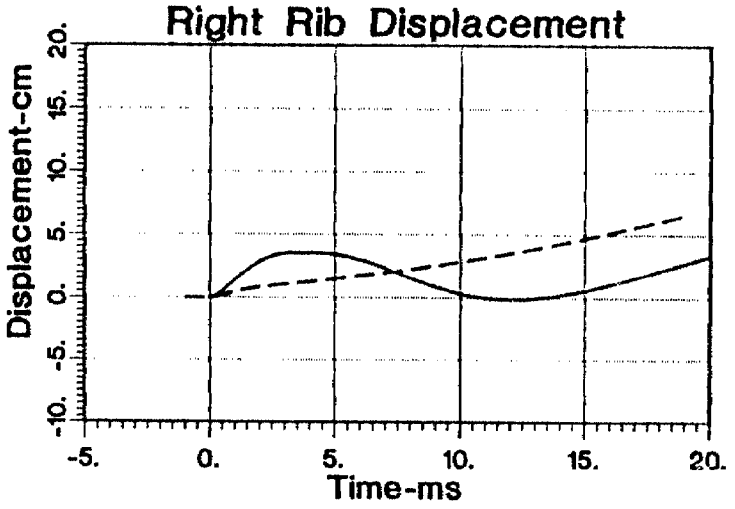

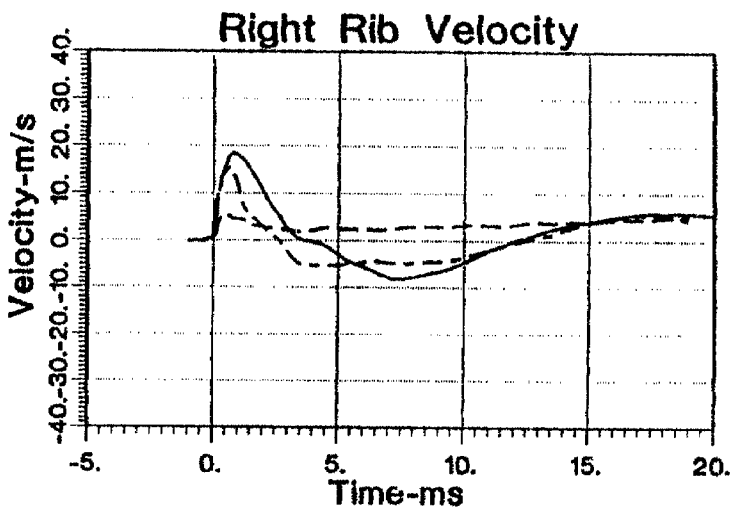

(a)

Figure 9. Case 2 Data Comparison

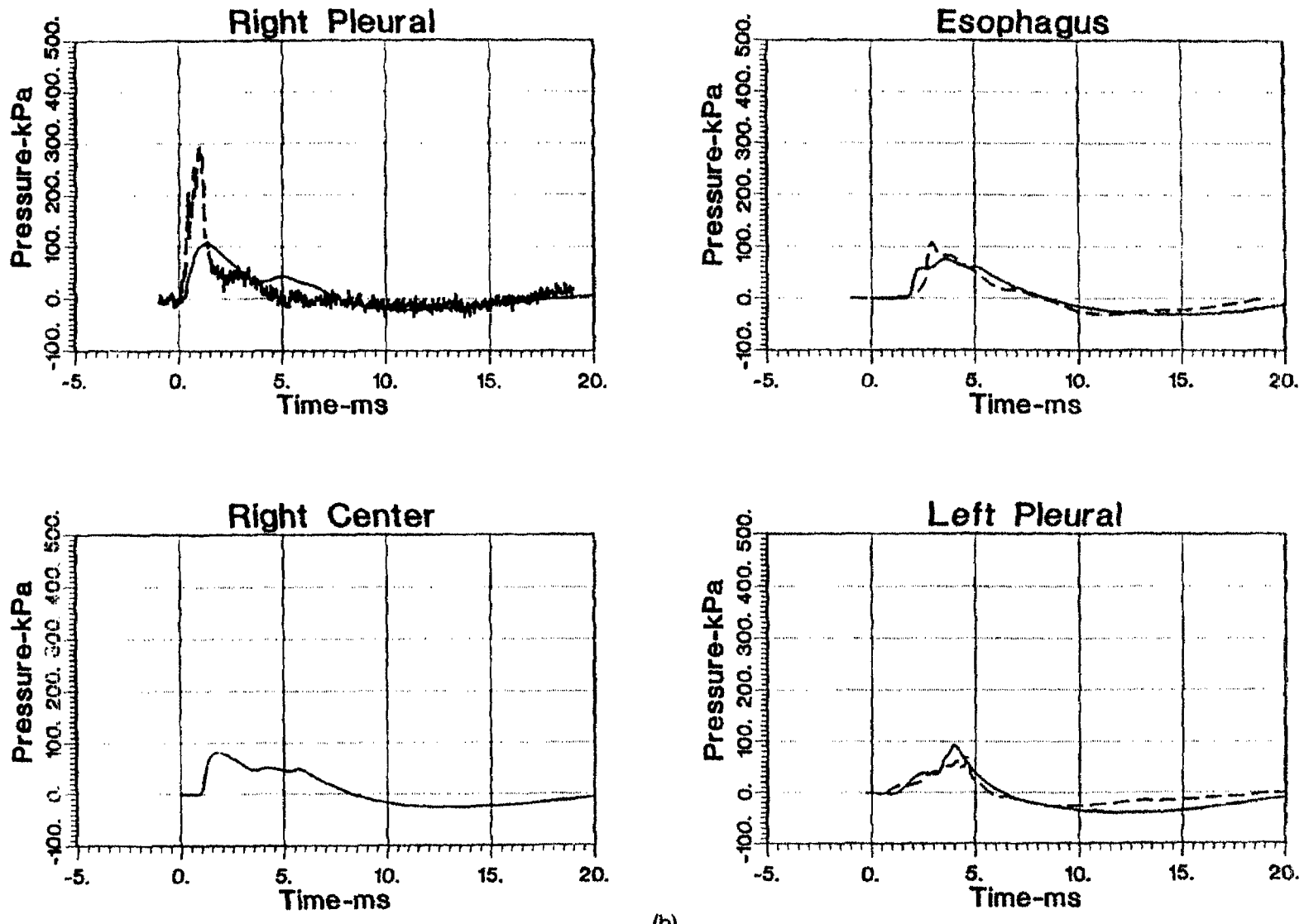

(b)

Figure 9. (Cont'd).

Freefield Shot: 1 lb C-4 at 0.8 ft HOB and 5.6 ft Range

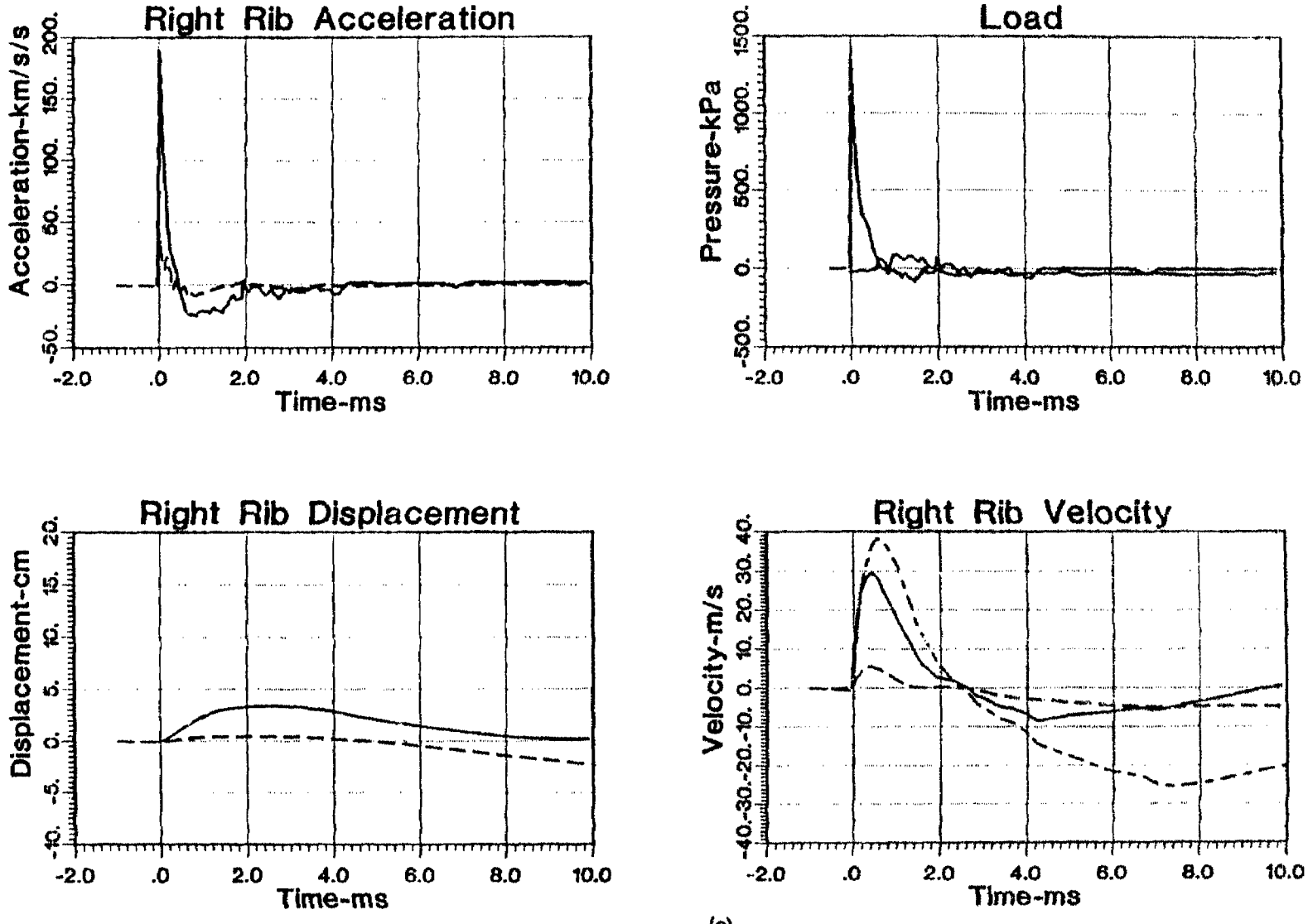

(a)

Figure 10. Case 3 Data Comparison

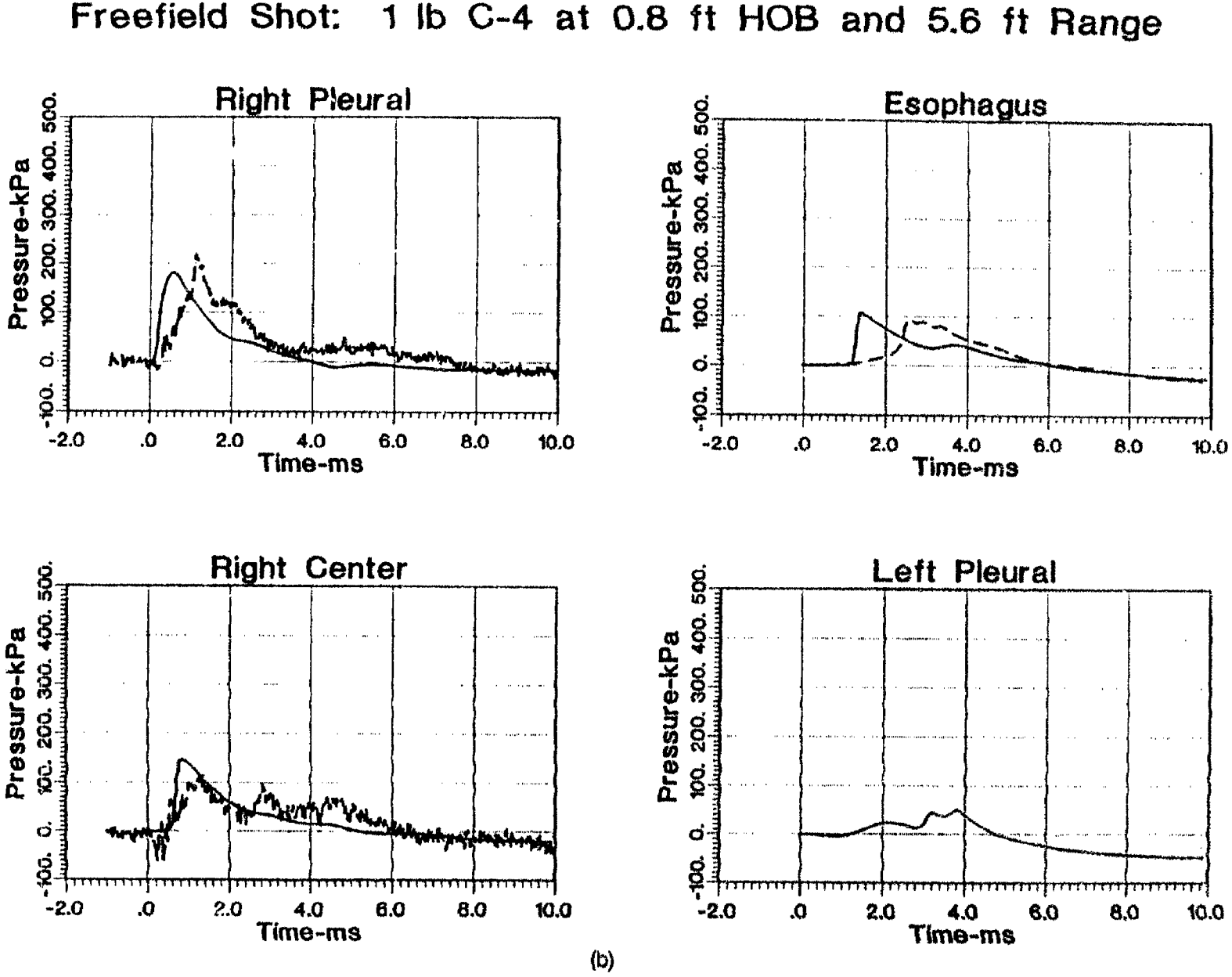

(b)

Figure 10. (Cont'd).

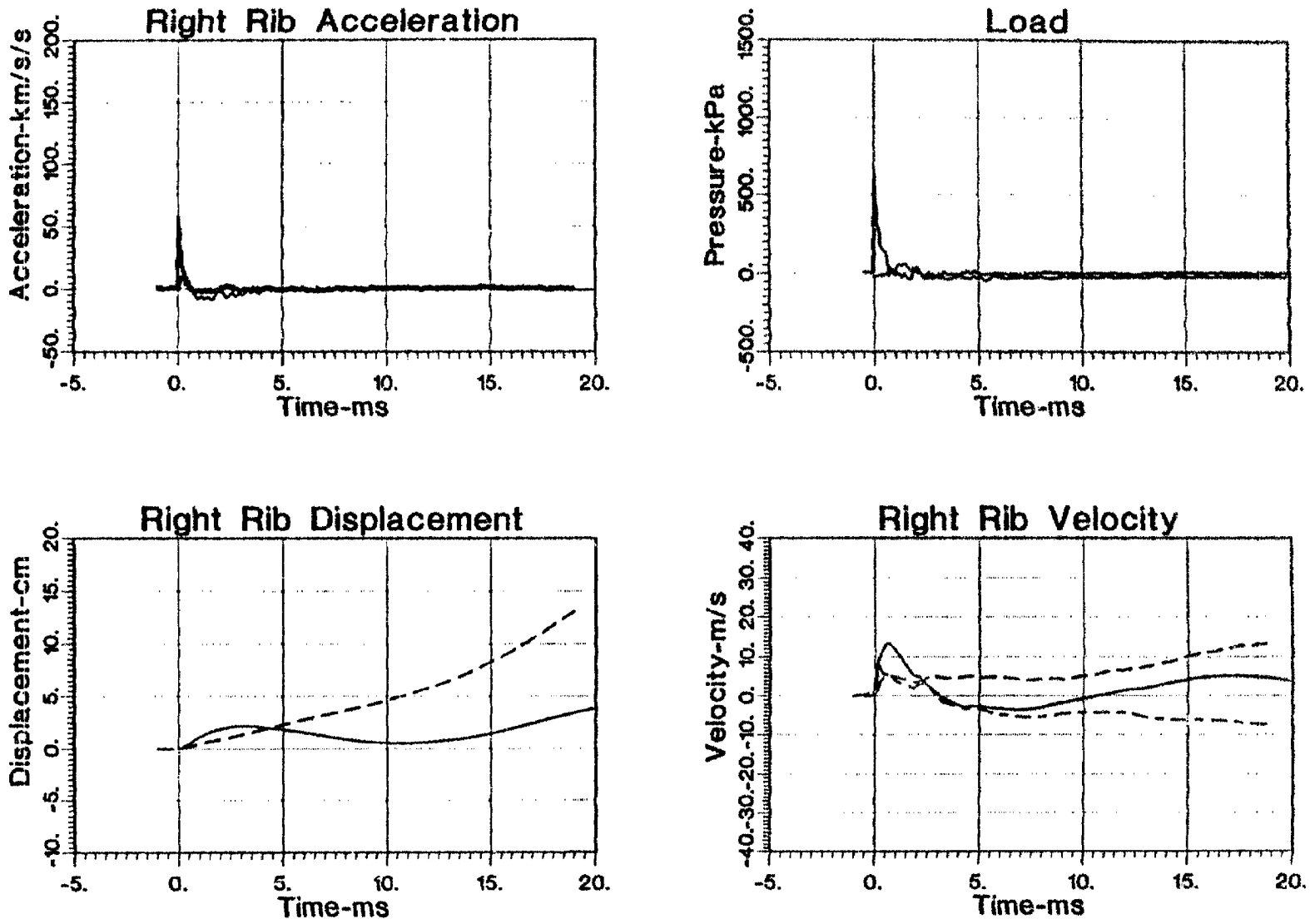

(a)

Figure 11. Case 4 Data Comparison

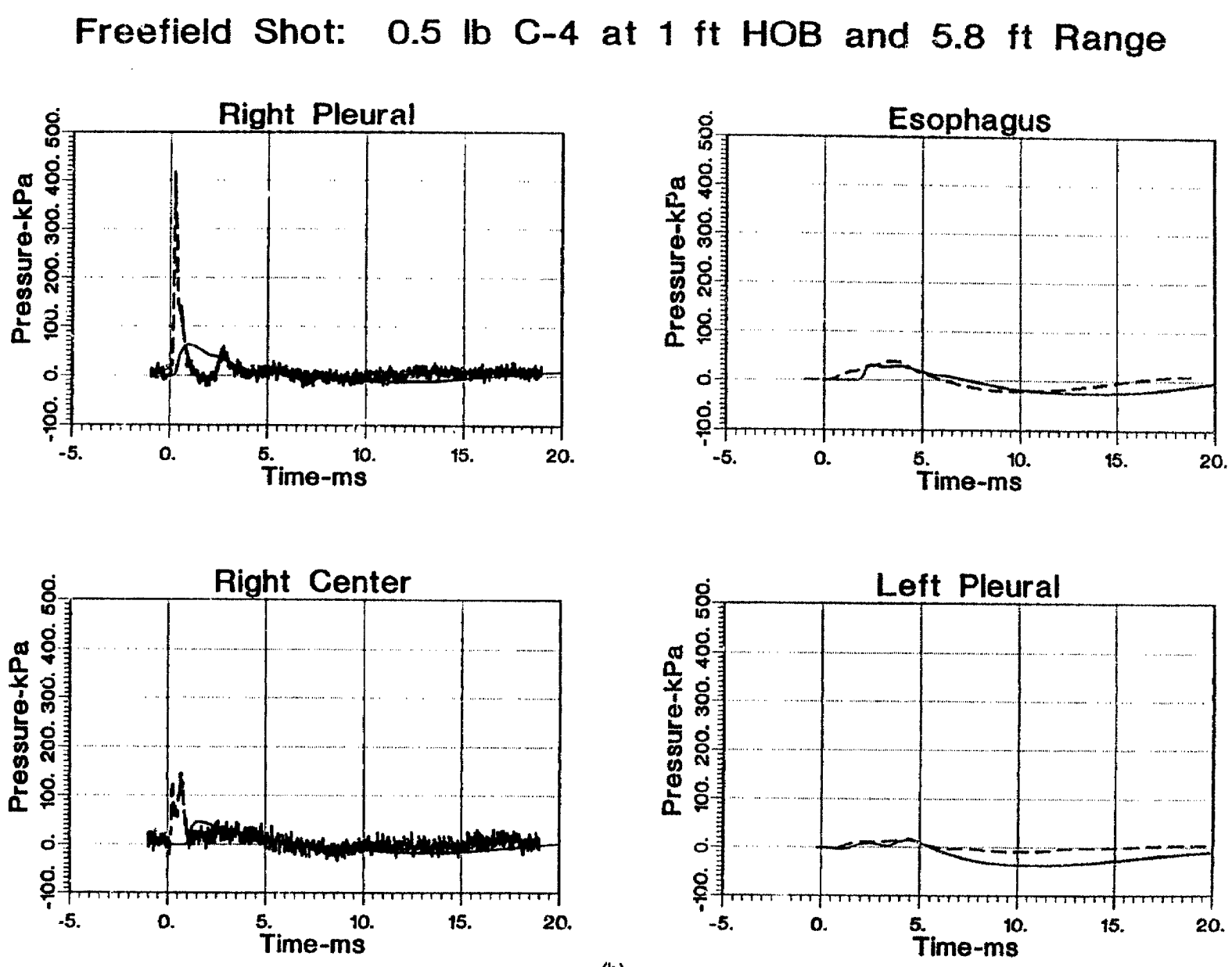

(b)

Figure 11. (Cont'd).

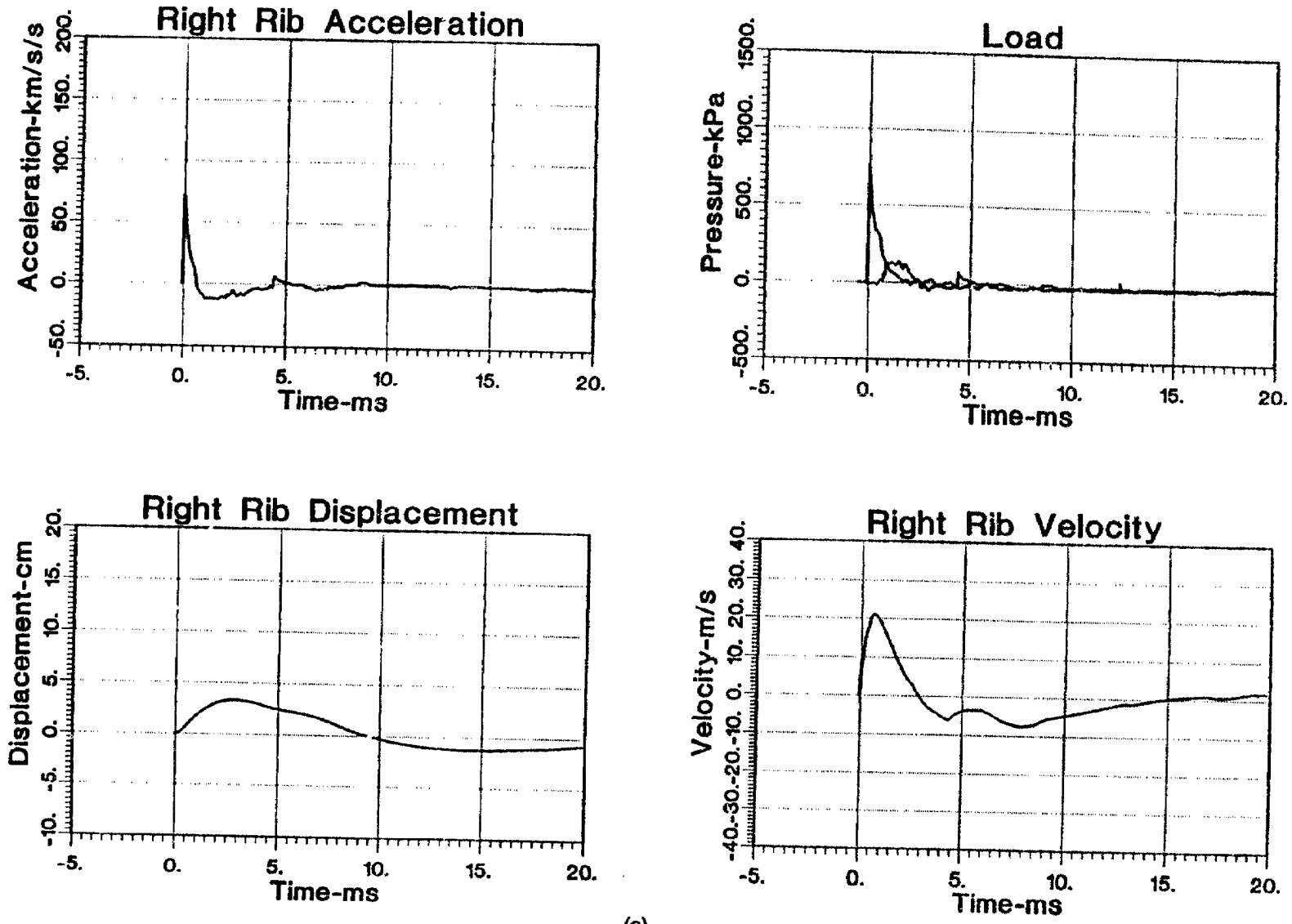

(a)

Figure 12. Case 5 Data Comparison

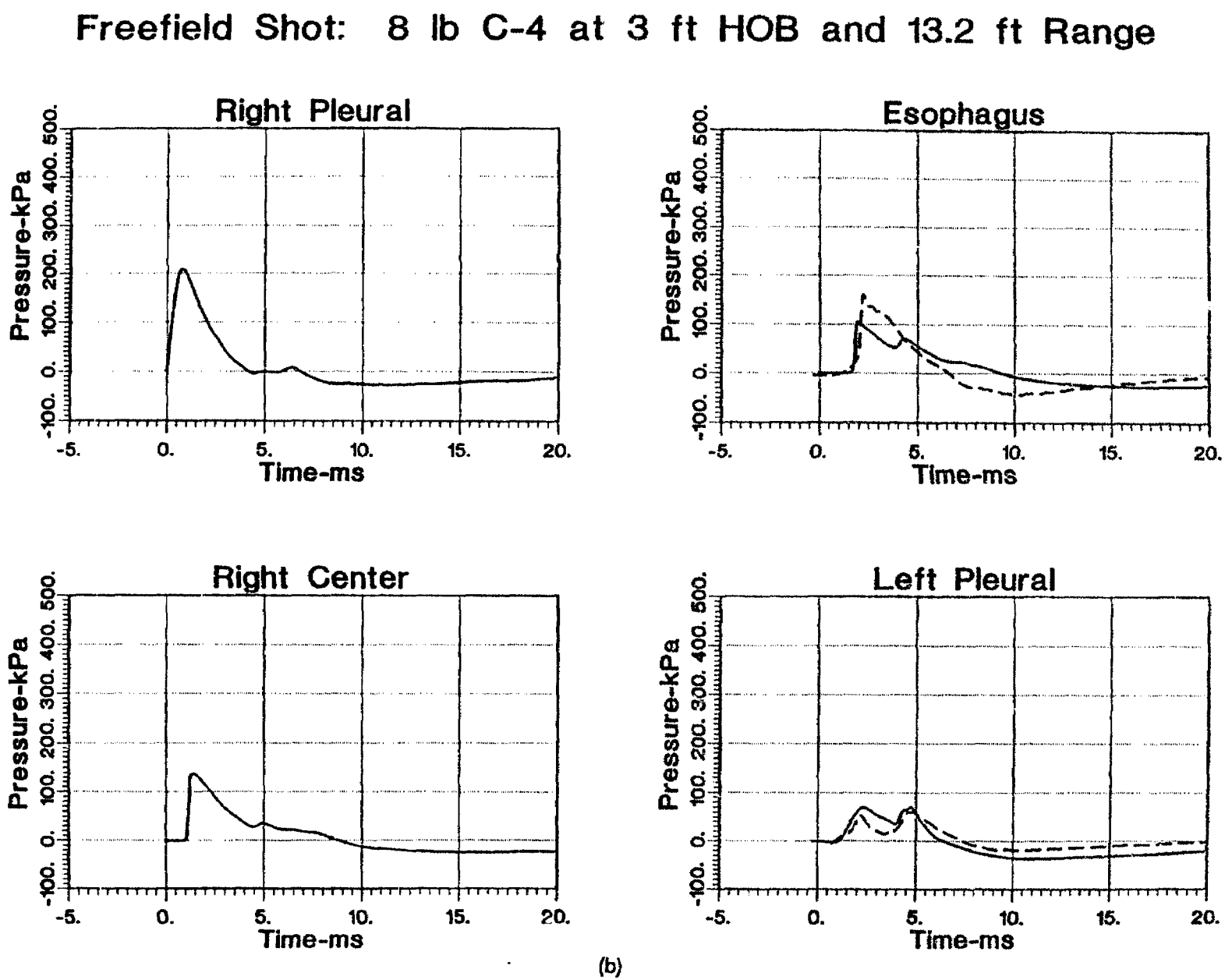

(b)

Figure 12. (Cont'd).

Freefield Shot: 8 lb C-4 at 2 ft HOB and 8.9 ft Range

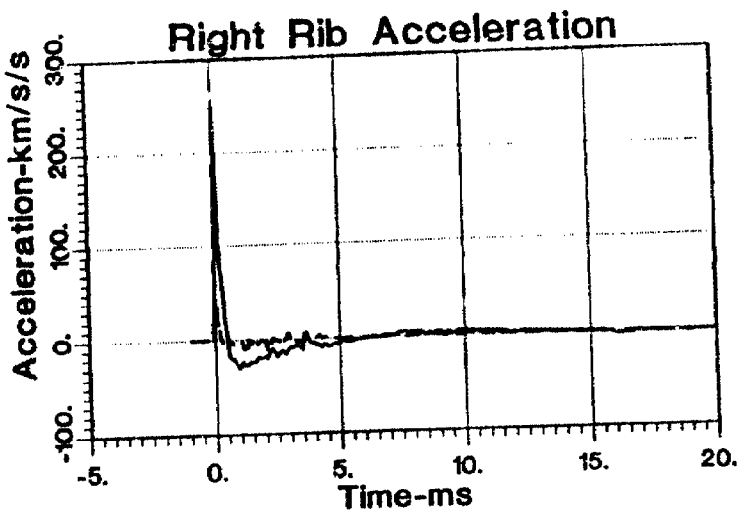

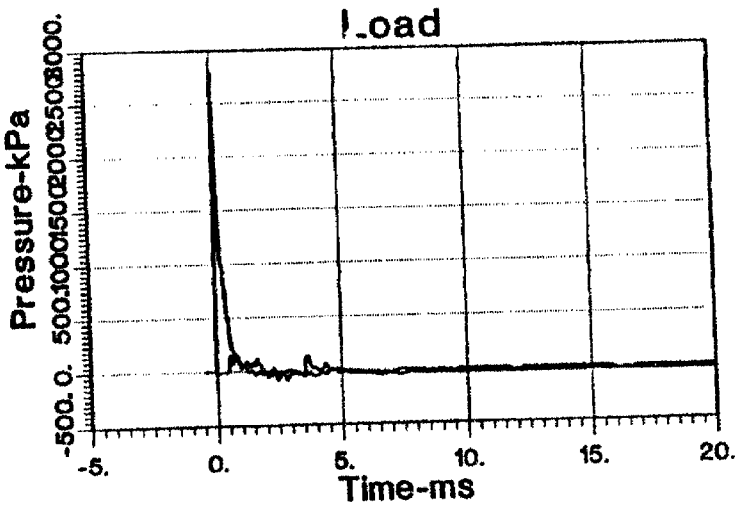

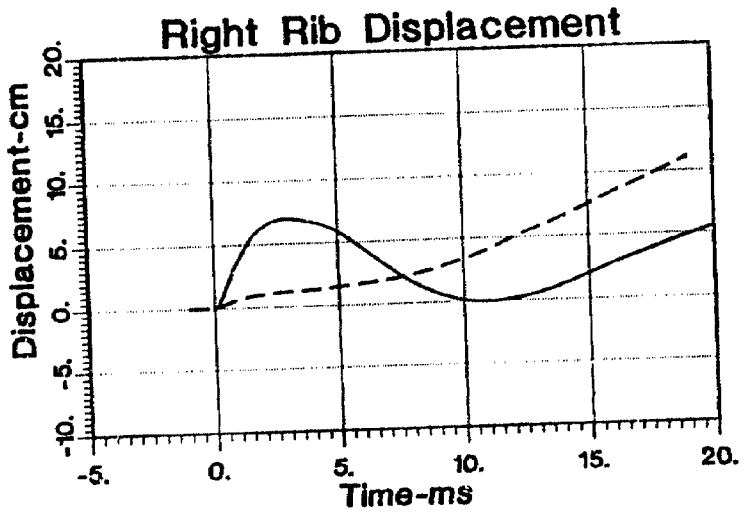

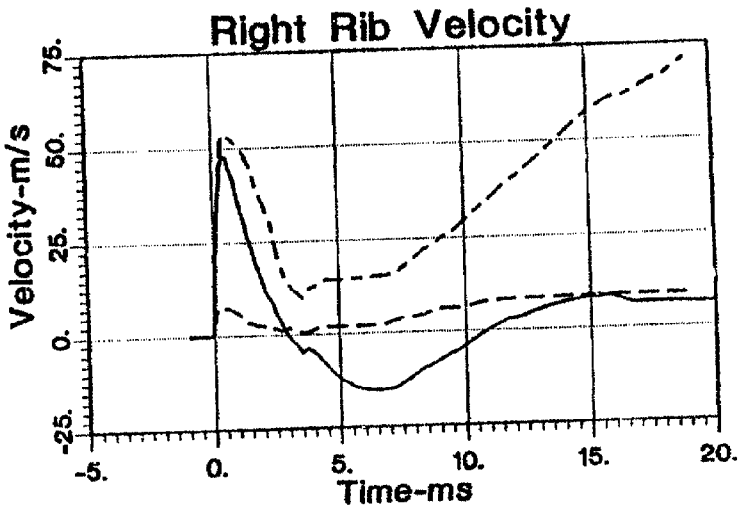

(a)

Figure 13. Case 6 Data Comparison

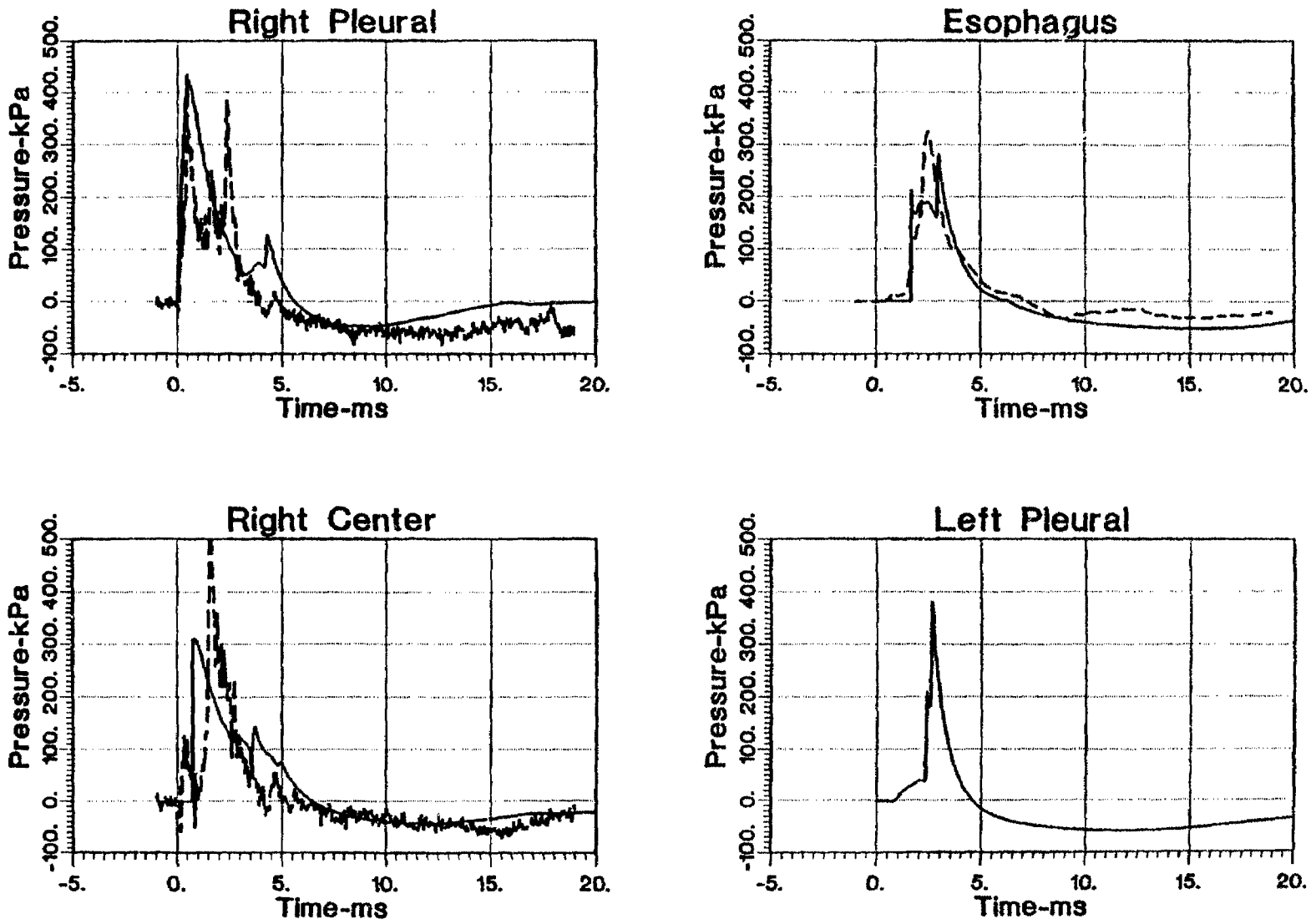

(b)

Figure 13. (Cont'd).

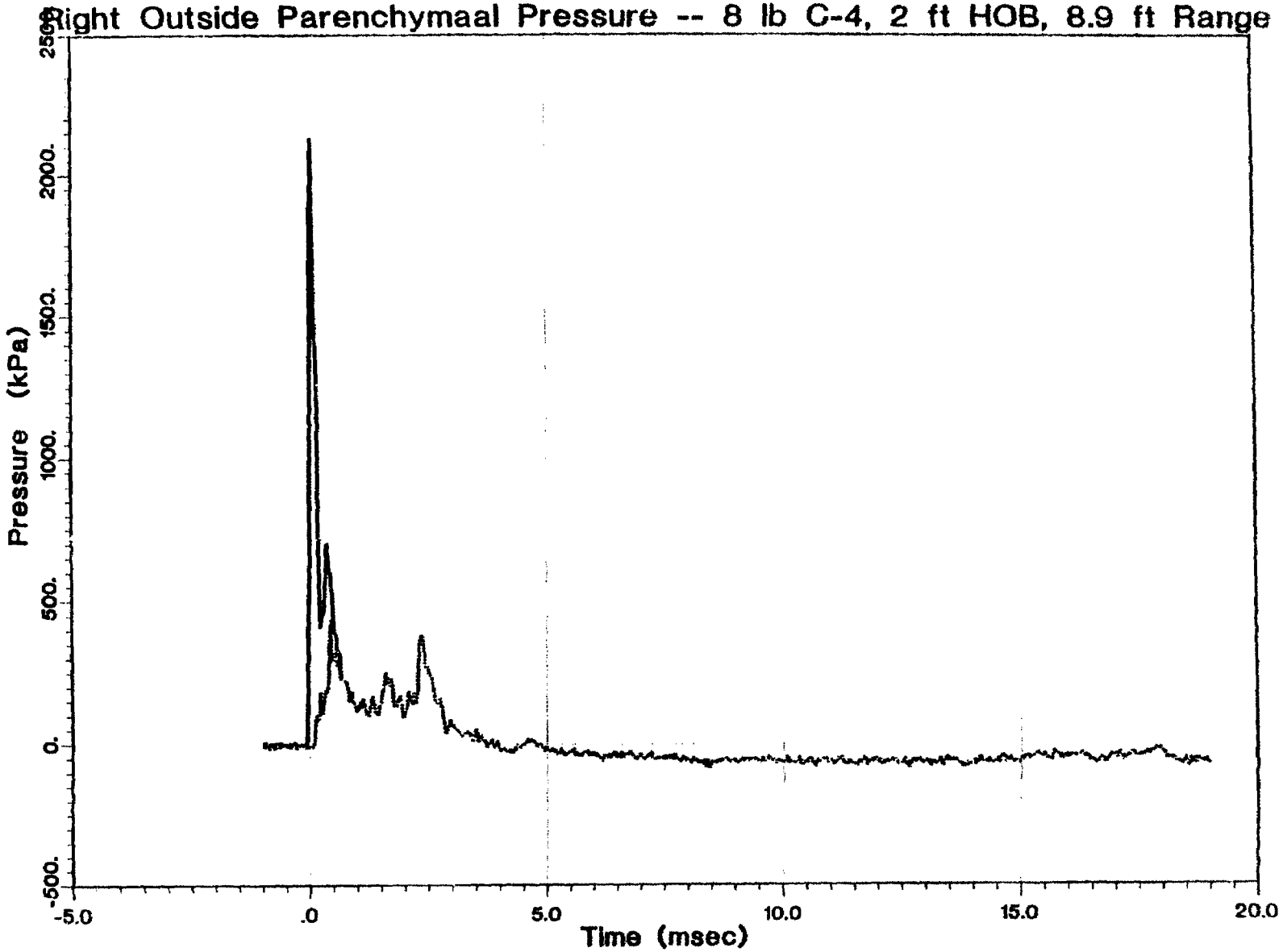

(c)

Figure 13. (Cont'd).

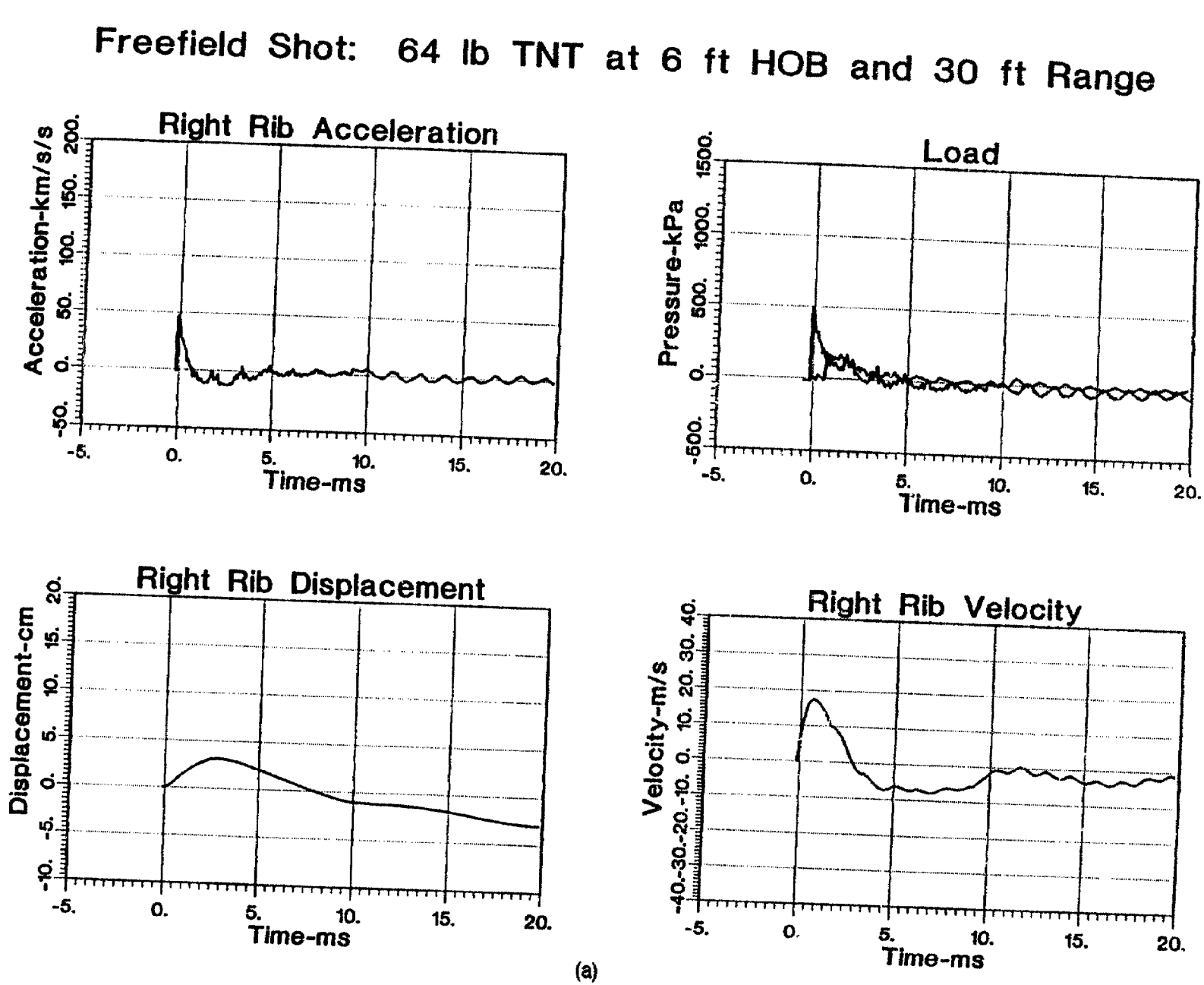

Figure 14. Case 7 Data Comparison

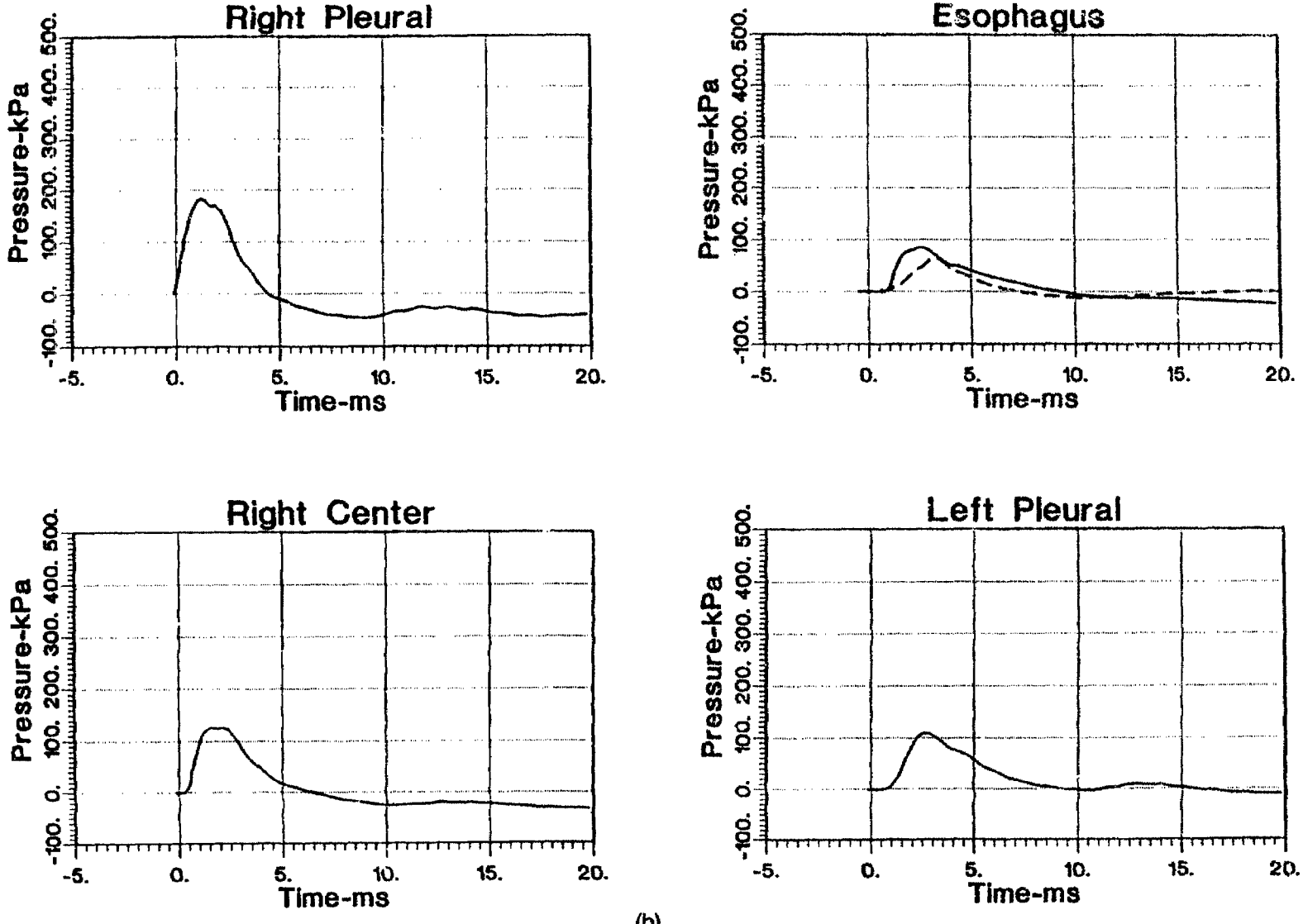

(b)

Figure 14. (Cont'd).

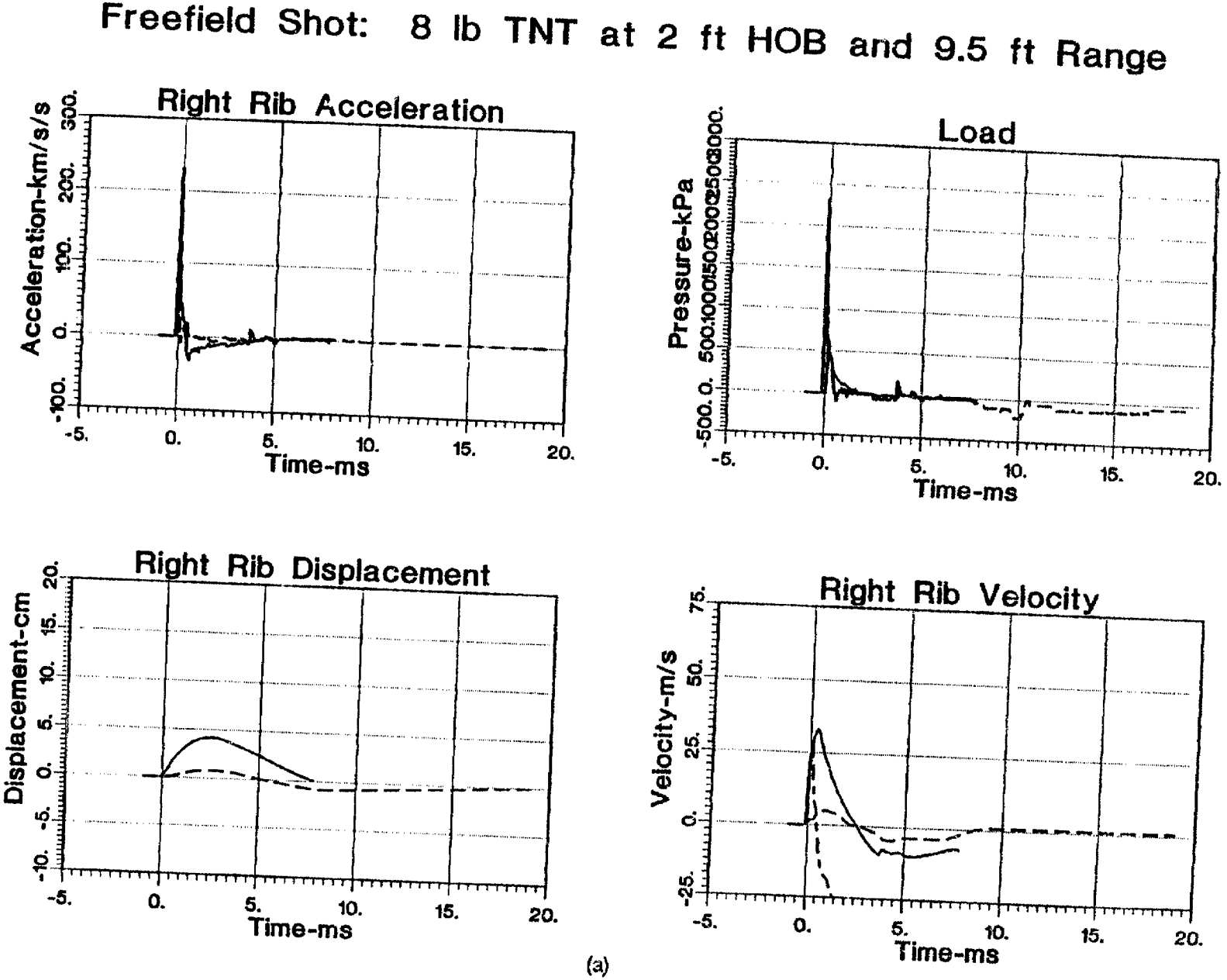

(a)

Figure 15. Case 8 Data Comparison

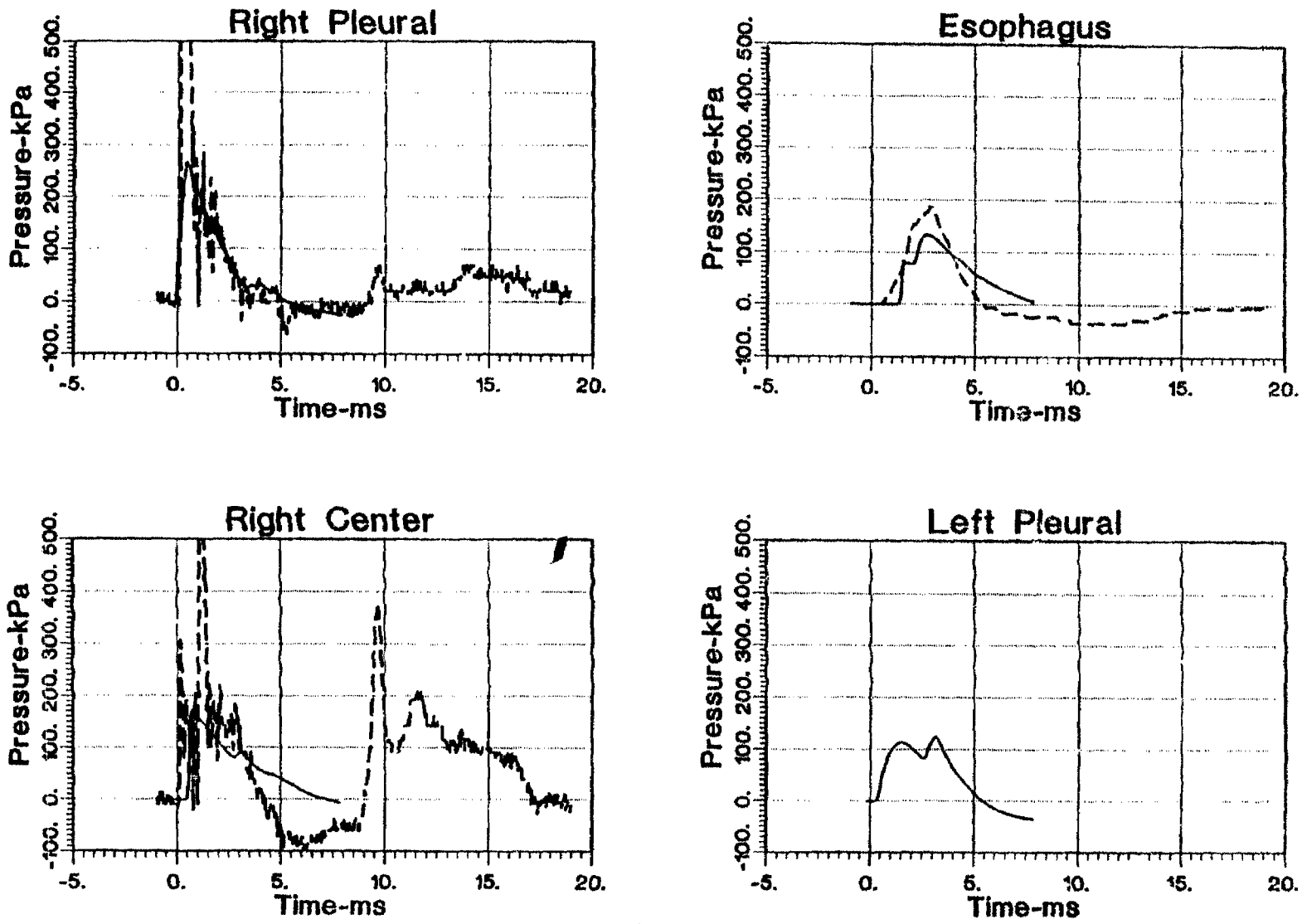

(b)

Figure 15. (Cont'd).

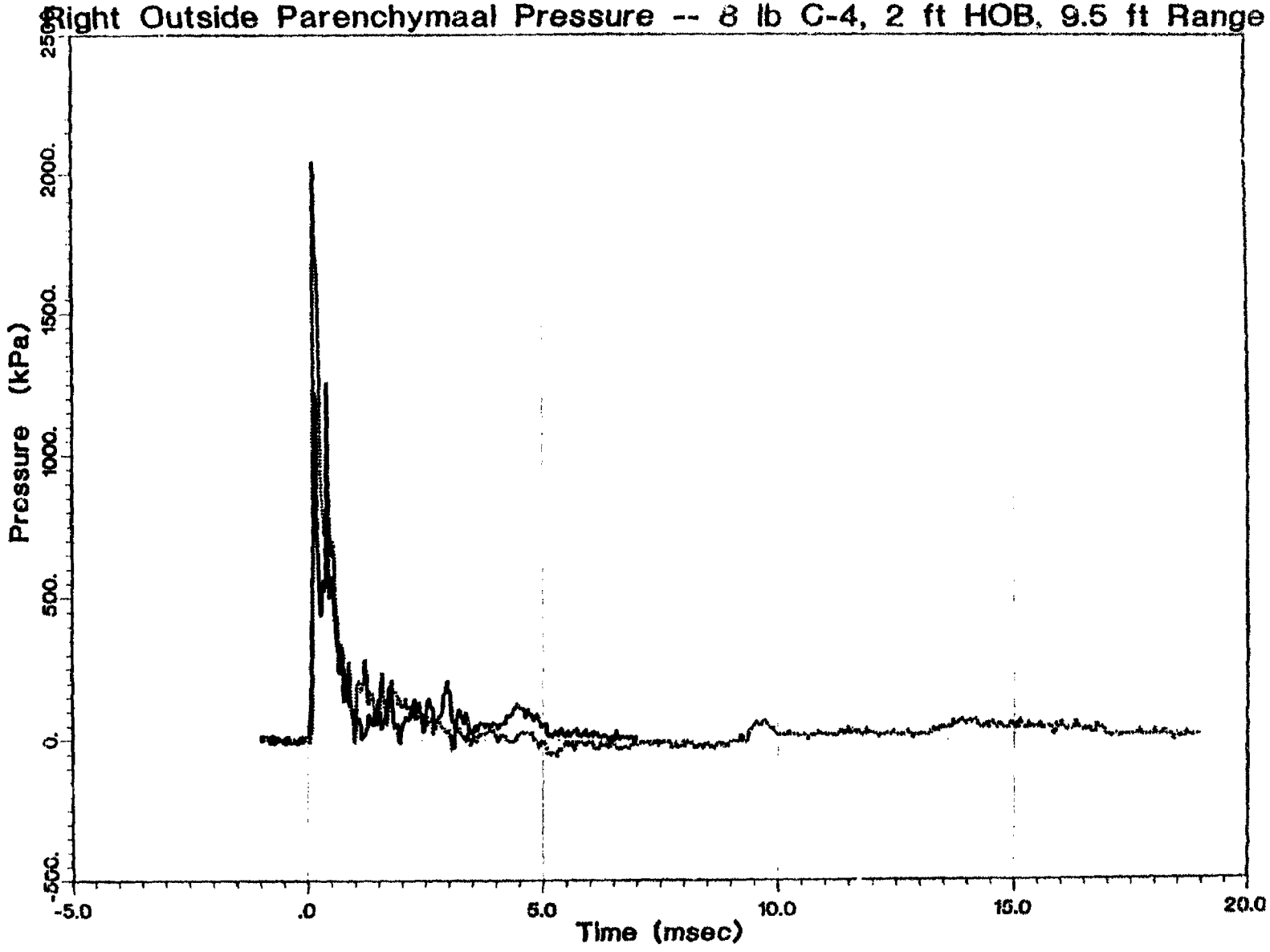

(c)

Figure 15. (Cont'd).

DATA INTERPRETATION

The free field blast wave first strikes the animal's right side producing a loading given by the LAMBDROID face-on blast side pressure gauge. The peak loading pressure can be two to five times the peak free field pressure for the range of cases evaluated. This loading accelerates the chest wall, transmitting a diminished pressure into the lung parenchyma as measured by the right parenchymal pressure gauge. Due to the inertia of the chest wall, the amplitude of the transmitted wave is significantly less than that of the load applied to the skin. The pressure wave then propagates from the pleural surface to the interior of the lung where it is met by a similar but lower intensity wave traveling from the left side of the animal. The left side wave is delayed from the right side wave by the time taken for the blast wave to travel around the animal from the right to left side, which is about a millisecond. The addition of the right and left side waves produces an esophageal pressure which may be higher than the parenchymal pressures.

Since the entire animal is subjected to the blast, one would expect pressure waves to be transmitted into the lung from all directions. However, inspection of the trans-parenchymal pressure data, suggests that the major contributions to the internal pressure come from the right and left sides with little contribution from the spine or the sternum. Since the spine is much more massive and rigid than the rib cage, the pressure wave formed just below the spine should be less intense than the waves produced by the ribs. In the case of the sternum, the distance from the abdomen to the diaphragm is about 18 cm. Hence the lung is well protected from the bottom by water filled organs and distance.

Measured intrathoracic pressures show an animal-to-animal variation. Figure 16 shows an ensemble of measured esophageal pressures for Case 8. Peak esophageal pressures for this case vary between 150 and 450 kPa. The lower pressure curves have longer rise times than the high pressure ones. Yu et al.[3] have made laboratory tests using the thorax surrogate and an esophageal surrogate which explain this variation. The esophageal surrogate, which is a tubular air filled balloon, is placed within the surrogate parenchymal material. The pressure signal inside the balloon has a lower peak and exhibits a longer rise time than the signal taken at the same position within the surrogate parenchymal material. Hence, the difference between the various esophageal measurements in the field tests shown in Figure 16 is explained by differences in the amount of air trapped around the pressure gauges in the esophagus.

There are also large animal-to-animal variations in the right outside, i.e., blast side, parenchymal pressures. Figure 17 shows pressure traces for three different animals sustaining Case 3 loads. Pressure gauges were inserted through the trachea and pushed in the bronchi. Some of the measured pressure difference may be due to air trapped around the gauges. However it is likely that the gauges are not all placed in the same location. For example if a gauge were placed lower in the lobe in the direction of the sternum, so that it was between the chest wall and the liver, Figure 1, then the measured pressure would be much larger.

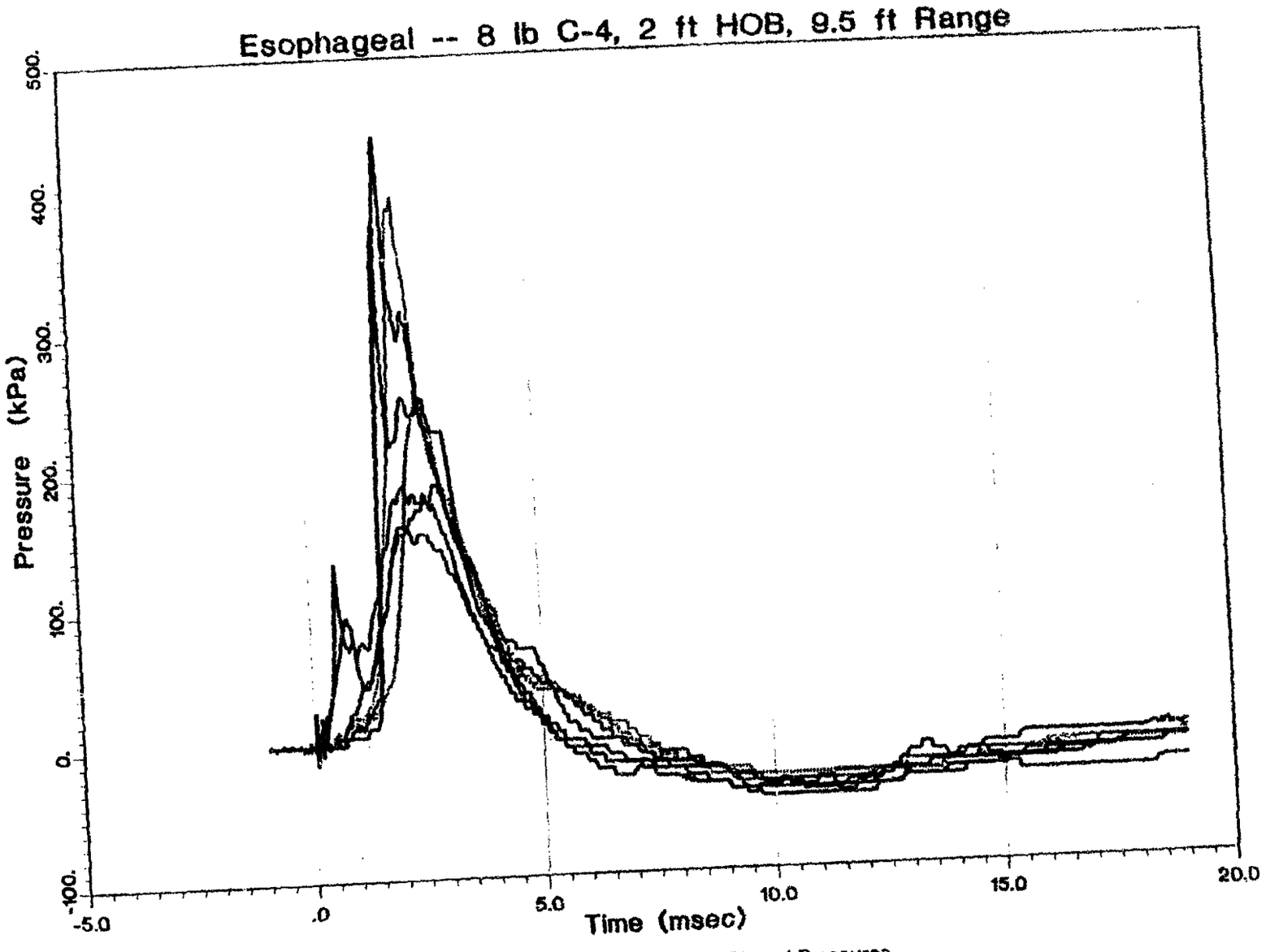

Figure 16. Ensemble of Measured Right Pleural Pressures

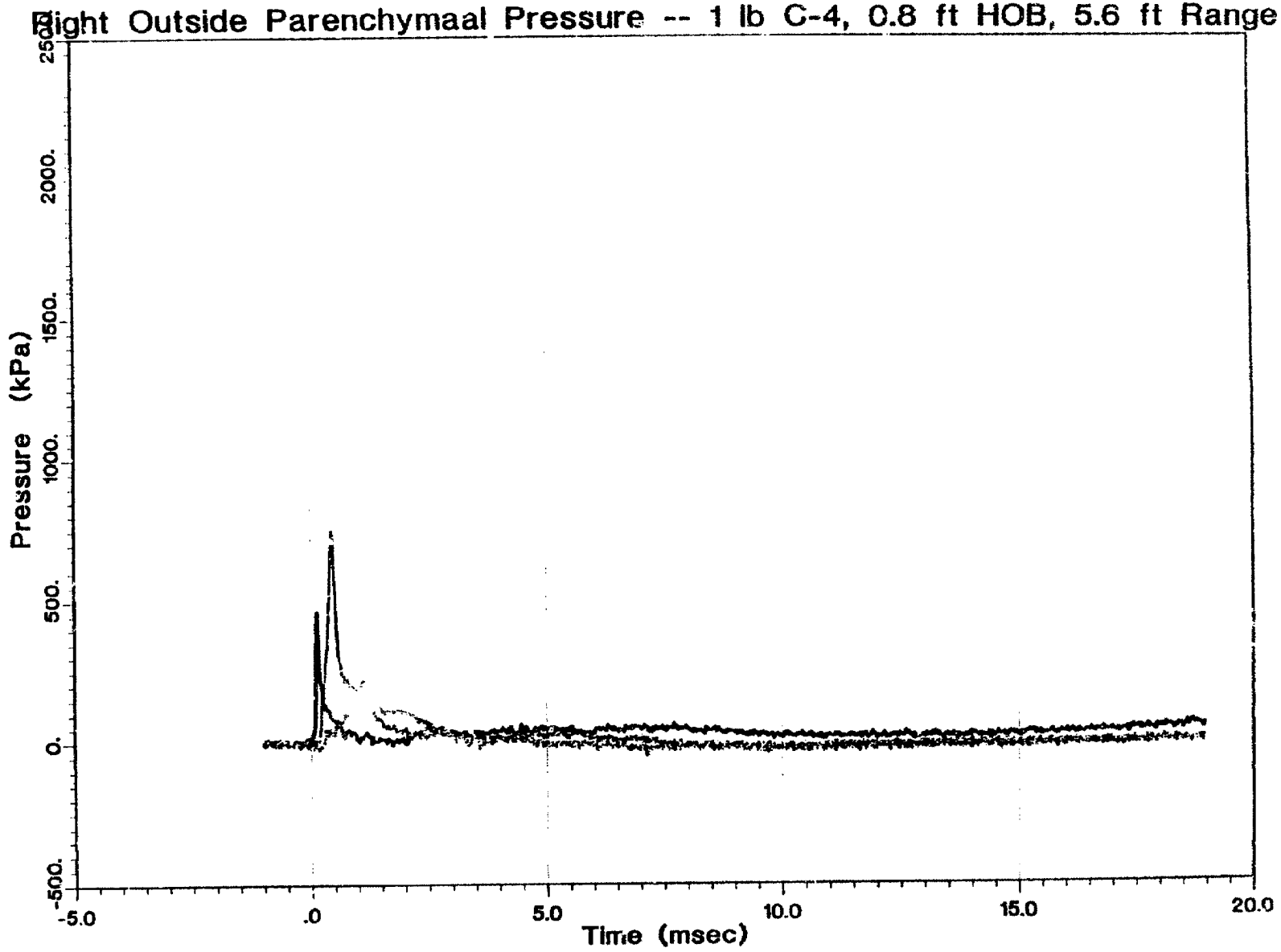

Figure 17. Ensemble of Measured Esophageal Pressures

CALCULATIONS

The key parameters needed to calculate the intrathoracic pressure are the animal geometry, pressure loading, mass of rib-muscle-skin layer, lung composite density, lung dissipation coefficient and ambient pressure at the test site. Numerical experiments compared to measured data indicate there is little or no contribution to the chest wall motion due to chest wall stiffness. Accordingly, the calculations presented here have the spring constant, k, set to zero for the chest wall.

Animal geometry and placement of pressure catheters was determined from x-rays taken during the field tests. The geometry data is given in Table 3. All the cross-sectional areas, A, are taken to be uniform with area 1 cm^2. Sixty finite difference cells were used to resolve the lung.

Measured data were used for the pressure loading, $p_r(t)$ and $p_l(t)$. Ambient air pressure, p^0, at Albuquerque, New Mexico was taken to be 82 kPa. The composite density of the lung, ρ, at normal inspiration was assumed to be 0.1 g/cm^3.

The parameter which was found to be of most importance to the development of the peak intrathoracic pressure was the chest wall mass per unit surface area, M_r. The blast loading on the skin causes the rib cage to accelerate inward, and the ribs, in turn, press against the lung setting up a pressure wave in the parenchyma. During the initial pulse of the loading, the acceleration is almost directly proportional to the loading force with constant of proportionality, M_r. In these calculations, the value of M_r was varied from 0.7 to 1.5 g/cm^2. The value used in each calculation is shown in Table 3. The true physical value of this parameter is unknown. However, since the distance from the sheep's skin to the pleural surface is usually between 1 and 2 cm, we would expect the mass per unit surface area of the rib/muscle layer to vary between 1 and 2 g/cm^2. No direct measurements of this quantity are available at this time, however it is reasonable to expect that there would be a sheep-to-sheep variation due to size and age.

Figures 8 through 15 show the comparison of calculations (solid lines) with measured data (dashed lines). Measured chest wall velocities calculated from Equation 25 using the measured pressure difference across the chest wall are shown as dotted dashed lines. Pressure loading and acceleration at the skin, four parenchymal pressures and the esophageal pressure are presented for each case when available. The physical blast conditions which define each of the eight cases are given in Table 1. Table 3 gives the parameters used in each of the calculations. A discussion of each case follows:

Case 1 Figure 8. 3 lb C-4 at 3.6 ft HOB, 16.1 ft range

Intrathoracic pressures and loads for this case were taken from 1985 data. No acceleration data is available for this case. The rib velocity calculated from the measured pressure difference across the chest wall agrees well with the calculated value until just after the first peak after which it is much higher. This corresponds to the difference in the measured and calculated right pleural pressure. Since the duration of the calculated pressure wave is longer, it will offer more resistance to the chest wall and slow it down faster. The agreement in the calculated and measured intrathoracic

pressures is good. The wave durations of the calculated pressure signals are a little longer than the measured ones.

Case 2 Figure 9. 3 lb C-4 at 3 ft HOB, 10.7 ft range

The peak measured acceleration and velocity are much lower than the calculated values. However the velocity computed from the measured pressure agrees well with the calculated velocity. This inconsistency occurs in most of the cases and suggests that the acceleration data is unreliable. The calculated right pleural pressure is much lower than the measured, however the other intrathoracic measurements agree well with the calculations. This may be due to the placement of the pressure catheter. Since this is the only right pleural data available for this case, please refer to the discussion of Case 3. as shown in Figure 17 which is an ensemble of all the available measured right pleural pressures for this case, there is a large shot to shot variation. which may be due to the placement of the catheter.

Case 3 Figure 10. 1 lb C-4 at 0.8 ft HOB, 5.6 ft range

Again, as in the previous case, the measured accelerations are low and inconsistent with the measured pressures. The intrathoracic pressures appear to be in fair agreement for this case. However the lowest of the three measured right pleural pressures, which are shown in Figure 17, was chosen for the comparison. In addition the calculation used a rib mass of 0.7 g/cm^2 for this case in order to increase the calculated peak right pleural pressure. As shown in Table 3, larger value was used in the other cases. A plausible hypothesis is that the large difference in the measured parenchymal pressures is due to difference in placement of the pressure gauges. If the gauges were placed in the tips of the lung lobes instead of at the level of the esophagus the pressures would be much larger. The measured peak esophageal pressure occurs later than the calculated one. Again, the calculation is probably using an incorrect placement.

Case 4 Figure 11. 0.5 lb C-4 at 1 ft HOB, 5.8 ft range

In this case the esophageal and left pleural pressures show good agreement. As before though, the measured right pleural pressures are much larger than the calculated ones. Correspondingly, the peak calculated velocity is higher than velocity found from the measured pressures.

Case 5 Figure 12. 8 lb C-4 at 3 ft HOB, 13.2 ft range

Only esophageal and left pleural measured data is available. They are in fair agreement with calculations. Better agreement in the peak esophageal pressure could be obtained by lowering the dissipation coefficient.

Case 6 Figure 13. 8 lb C-4 at 2 ft HOB, 8.9 ft range

With the exception of the right center parenchymal pressure, the measured and calculated values show good agreement for this case. However as shown in the last graph of Figure 12, the lowest right parenchymal measurement was used to make the comparison. Please refer to the discussion for Case 3.

Case 7 Figure 14. 64 lb TNT at 6 ft HOB, 30 ft range

Only measured esophageal data is available for this case. It is in fair agreement with the calculation.

Case 8 Figure 15. 8 lb TNT at 2 ft HOB, 9.5 ft range

The measured esophageal pressure is in good agreement with the calculated values. However, as in some of the previous cases, the measured right pleural and right center pressures are much higher than the calculated ones. The last graph of Figure 15 shows the available measured right pleural pressures.

Measured chest wall accelerations are usually lower than those calculated. However the measured accelerations are inconsistent with the measured pressure when both are integrated using Equation 25 to find the chest wall velocity.

The one-dimensional model exhibits the correct wave propagation from the right pleural surface through to the left pleural surface. However in many cases the calculated right side parenchymal pressures are too low. This may be due to a lack of knowledge about the exact placement of the pressure gauges within the lung.

Measured esophageal data shows a longer rise time than the calculated results. This is because the esophagus is presently modeled as lung parenchyma when in fact it is a tube with air trapped inside.

SUMMARY

The one-dimensional model has provided insight into the mechanical response of the lung to blast loading. The key physical parameters are the rib/muscle mass per unit area, the composite density of the lung at normal respiration and the coefficient of dissipation within the lung. Generally, the model predictions are in good agreement with measurement and should eventually allow reduced animal testing and better prediction of injury circumstances.

REFERENCES

1. Dodd, K. T., M. J. Vander Vorst, K. C. O'Hair, Y. Y. Phillips, "Analysis of Field Test Results of the Internal Mechanical Response of Sheep to Blast Loading," Proceedings of the Third Workshop on Launch Blast Overpressure, Ballistic Research Laboratory, Aberdeen Proving Ground, Maryland, June 1986.

2. Dodd, K. T., "Analysis of Field Test Results of the Biophysical Response of Sheep to Blast Loading," Proceedings of the Tenth International Symposium of Military Applications of Blast Simulation, Bad Reichenhall, West Germany, September 1987.

3. Yu, J. H.-Y., K. H.-H. Ho, J. H. Stuhmiller, "A Surrogate Model of Thoracic Response to Blast Loading," August 1989.

4. Yu, J. H.-Y., E. J. Vasel, and J. H. Stuhmiller, "Design and Field Test of a Blast Overpressure Test Module," JAYCOR Technical Report, August 1989.

5. Vander Vorst, M. J. and C. A. Meister, "VU Users Manual, Version 1.6," JAYCOR Technical Report, August 1989.

DISTRIBUTION LIST

4 copies	Director Walter Reed Army Institute of Research ATTN: SGRD-UWZ-C Washington, DC 20307-5100
1 copy	Commander US Army Medical Research and Development Command ATTN: SGRD-RMI-S Fort Detrick, Frederick, MD 21701-5012
2 copies	Defense Technical Information Center (DTIC) ATTN: DTIC-DDAC Cameron Station Alexandria, VA 22304-6145
1 copy	Dean School of Medicine Uniformed Services University of the Health Sciences 4301 Jones Bridge Road Bethesda, MD 20814-4799
1 copy	Commandant Academy of Health Sciences, US Army ATTN: AHS-CDM Fort Sam Houston, TX 78234-6100